dynamic software & engineering

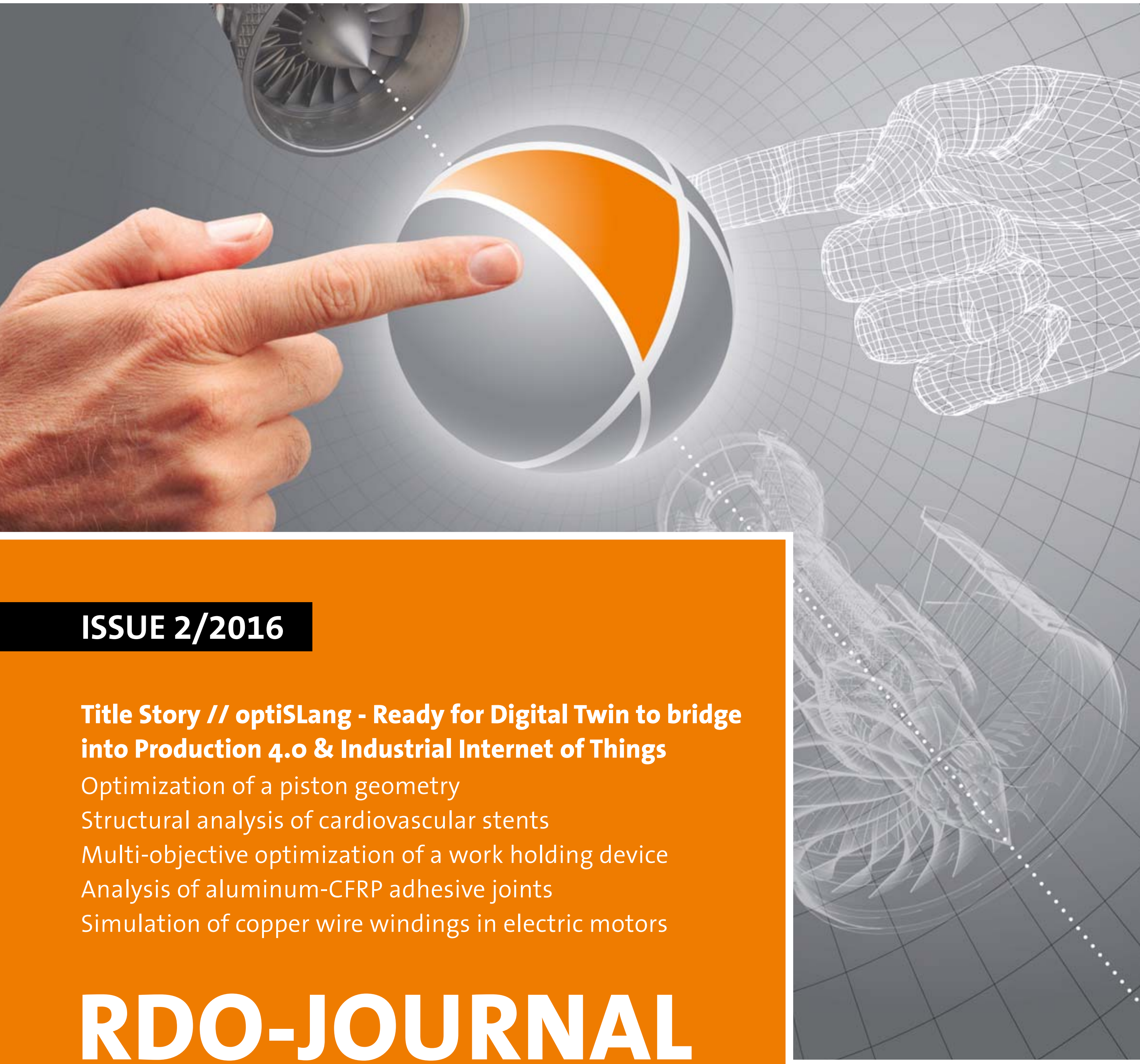

ISSUE 2/2016

Title Story // optiSLang - Ready for Digital Twin to bridge into Production 4.0 & Industrial Internet of Things

Optimization of a piston geometry

Structural analysis of cardiovascular stents

Multi-objective optimization of a work holding device

Analysis of aluminum-CFRP adhesive joints

Simulation of copper wire windings in electric motors

RDO-JOURNAL

optiSLang

multiPlas

ETK

SoS

OPTISLANG - READY FOR DIGITAL TWIN TO BRIDGE INTO PRODUCTION 4.0 & INDUSTRIAL INTERNET OF THINGS

Production 4.0 along with the Industrial Internet of Things are creating massive opportunities for companies to improve their products and services with the help of simulation models. Parametric simulation models and digital twins will become part of a Product Lifecycle Management (PLM) platform. Thus, very valuable assistance systems will be developed to support engineers by evaluating and visualizing information comprehensibly for making decisions in the design process, to optimize operation and maintenance of products and processes or solving urgent problems on short notice in operating modes.

CAE-based product development approaches are indispensable for fulfilling the idea of Production 4.0 and the Internet of Things. Within a modular structured PLM, cyber-physical systems monitor processes and create a virtual copy of the product. A so called "Digital Twin" refers to a computerized companion of a physical design simulating product operation performance or representing near real-time status and working conditions. This approach can be used for monitoring, diagnostics and prognostics helping to improve the performance and reliability of products. Also, the development of intelligent maintenance systems can leverage the use of digital twins by finding the root causes and effects in operating status. There is no doubt that Production 4.0 and the Internet of Things represent one of the largest sources of revenue growth for the future.

Of course, the complexity of connected PLM Management in both the product and its operating environment also generates a set of non-trivial engineering challenges. For example, the ability of these information systems to calibrate a "Digital Twin" requires the aggregation of raw data to higher-value context information. Here, optiSLang supports the identification of important model parameters for the best fit between simulation and measurement.

In the various phases of Product Development Processes (PDPs), optiSLang can play a vital role in virtual product optimization, generation of parametric models and workflows as well as in the calibration of virtual models to tests. Thus, optiSLang is capable to bridge the gap between modern Product Lifecycle Management (PLM) systems and individual product development hubs.

The title story of this journal will give a brief overview on the integration of optiSLang within and beyond CAx Processes and Product Lifecycle Management systems.

Apart from that, we again have selected case studies and customer stories concerning CAE-based Robust Design Optimization (RDO) applied in different industries.

I hope you will enjoy reading our magazine.

Yours sincerely

Johannes Will
Managing Director DYNARDO GmbH

Weimar, September 2016

CONTENT

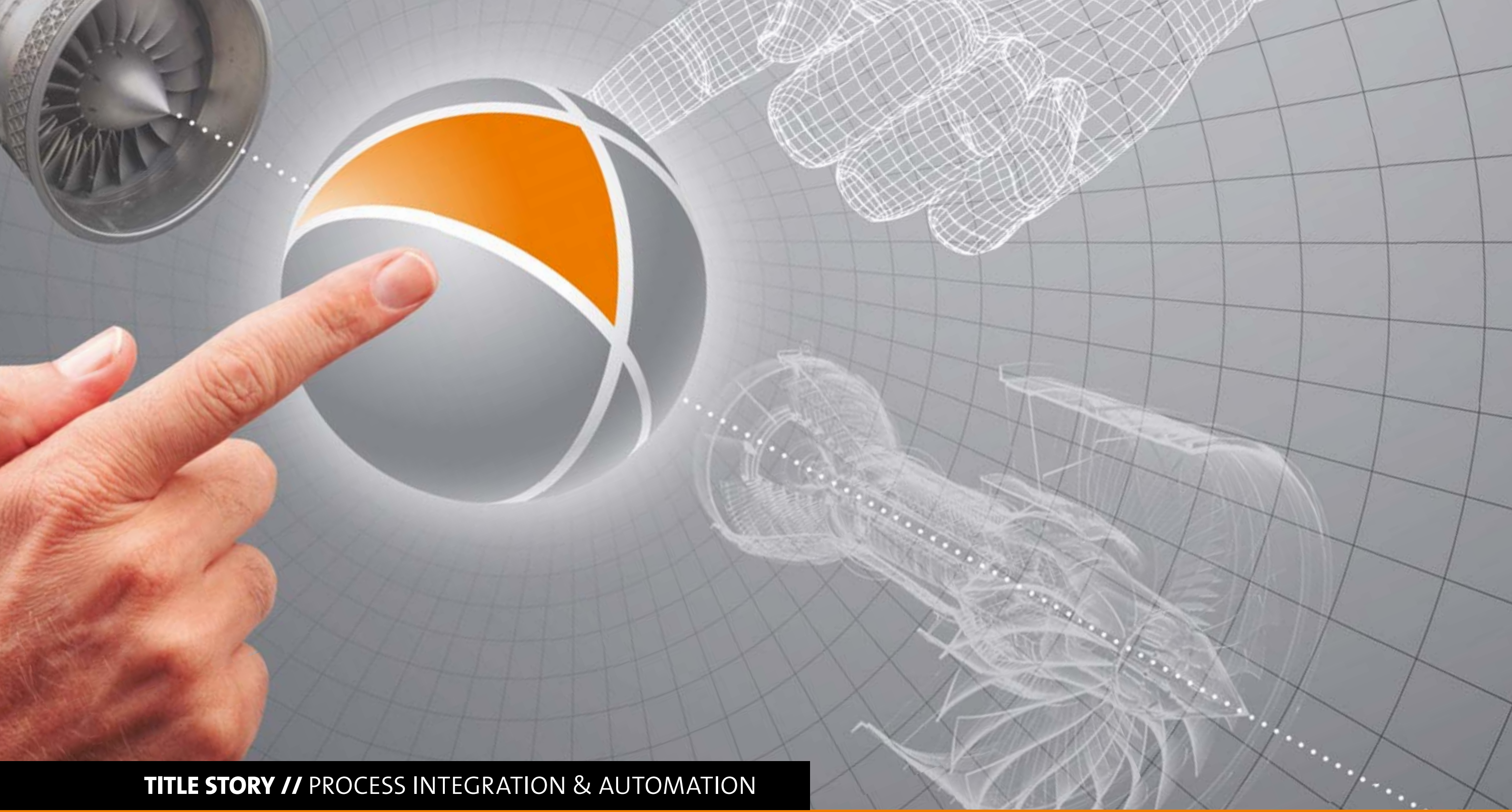

OPTISLANG - READY FOR DIGITAL TWIN TO BRIDGE INTO PRODUCTION 4.0 & INTERNET OF THINGS

optiSLang is capable to bridge the gap between modern Product Lifecycle Management (PLM) systems and individual product development hubs.

Motivation

The new generation of process automation within Industry 4.0 has transformed the scope of Business Process Models (BPM) for leading global manufacturers. With tools such as Virtual Manufacturing Execution Systems, Cloud Computing and Big Data Analytics, the Internet of Things (IoT) is becoming a modern and efficient umbrella of planning, processing, feedback and control systems, paving the way for the next generation of smart designs and manufacturing systems.

Within the scope of Industry 4.0, there has been a widespread development of standalone tools, each offering special solutions to underlying problems and requiring software specific know-how. While the number of standalone modules and corresponding software vendors have increased, the advent of IT-HPC and Big Data has led to enormous amount of data generation and necessitated the need for an integrated data evaluation and management system. Integration of modern simulation processes could open up even further opportunities into optimization and control of such systems. It would enable to speed up the decision-making process, enhance traceability and improve existing Quality Management Systems (QMS) in place. It should be noted, however, that simulation technology is not an IoT product itself but is proving to be a pivotal driver of IoT processes in the future.

In the various phases of Product Development Processes (PDPs), optiSLang is capable to play a vital role to shorten production cycles, deliver enhancements and resolve conflicts with respect to quality, product robustness and costs. Apart from optimizing individual process workflows within various stages of PDPs, optiSLang could be used to bridge the gap between modern Product Lifecycle Management (PLM) systems and individual product development hubs. Here we look at optiSLang's potential role at various process stations such as:

- Design of Experiment, Software-in-Loop (SiL) and Hardware-in-Loop (HiL) integrations
- Statistical Analysis
- Databased ROM
- Virtual Product Optimization
- Generation of parametric models and workflows
- Calibration of virtual models to tests
- Robust Design Optimization (RDO)

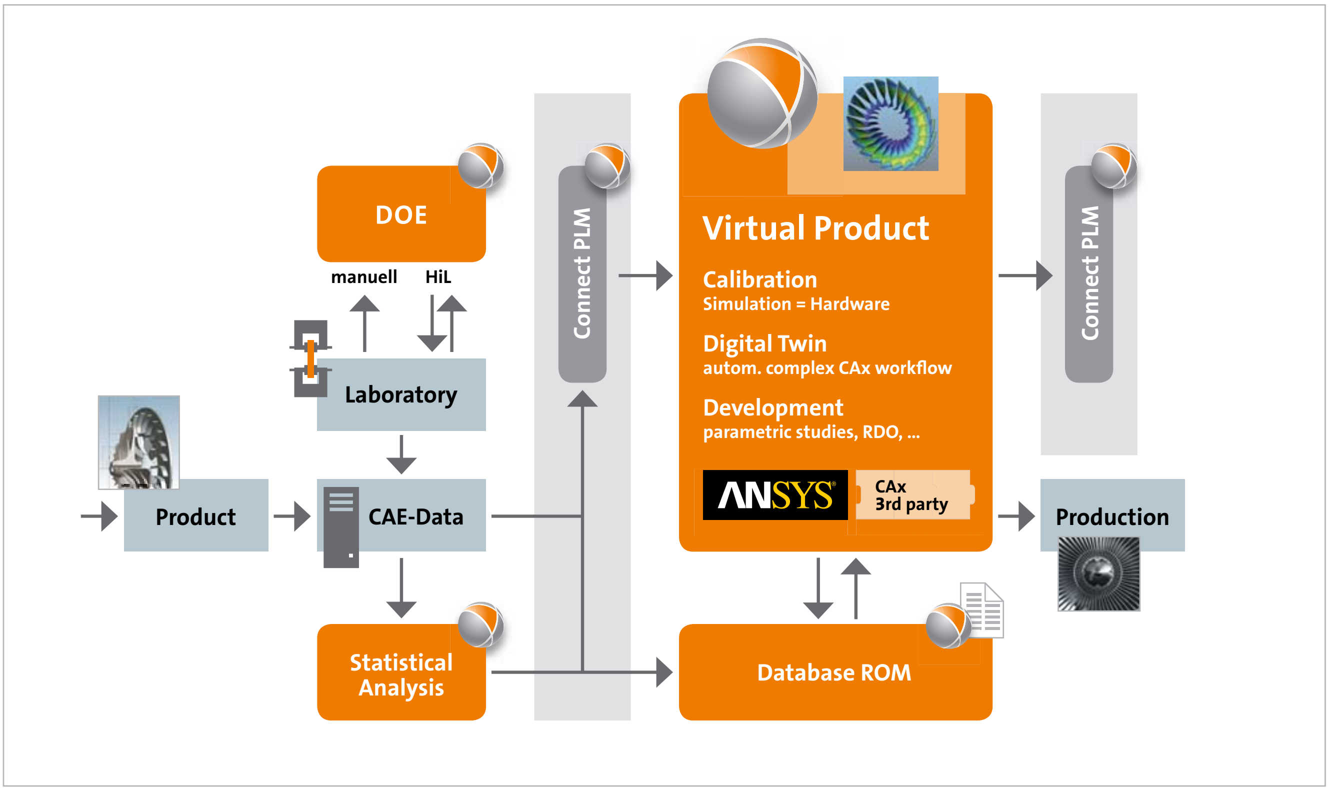

Fig. 1: Integration of optiSLang within and beyond CAx Processes, Product Lifecycle Management and Hardware-in-Loop

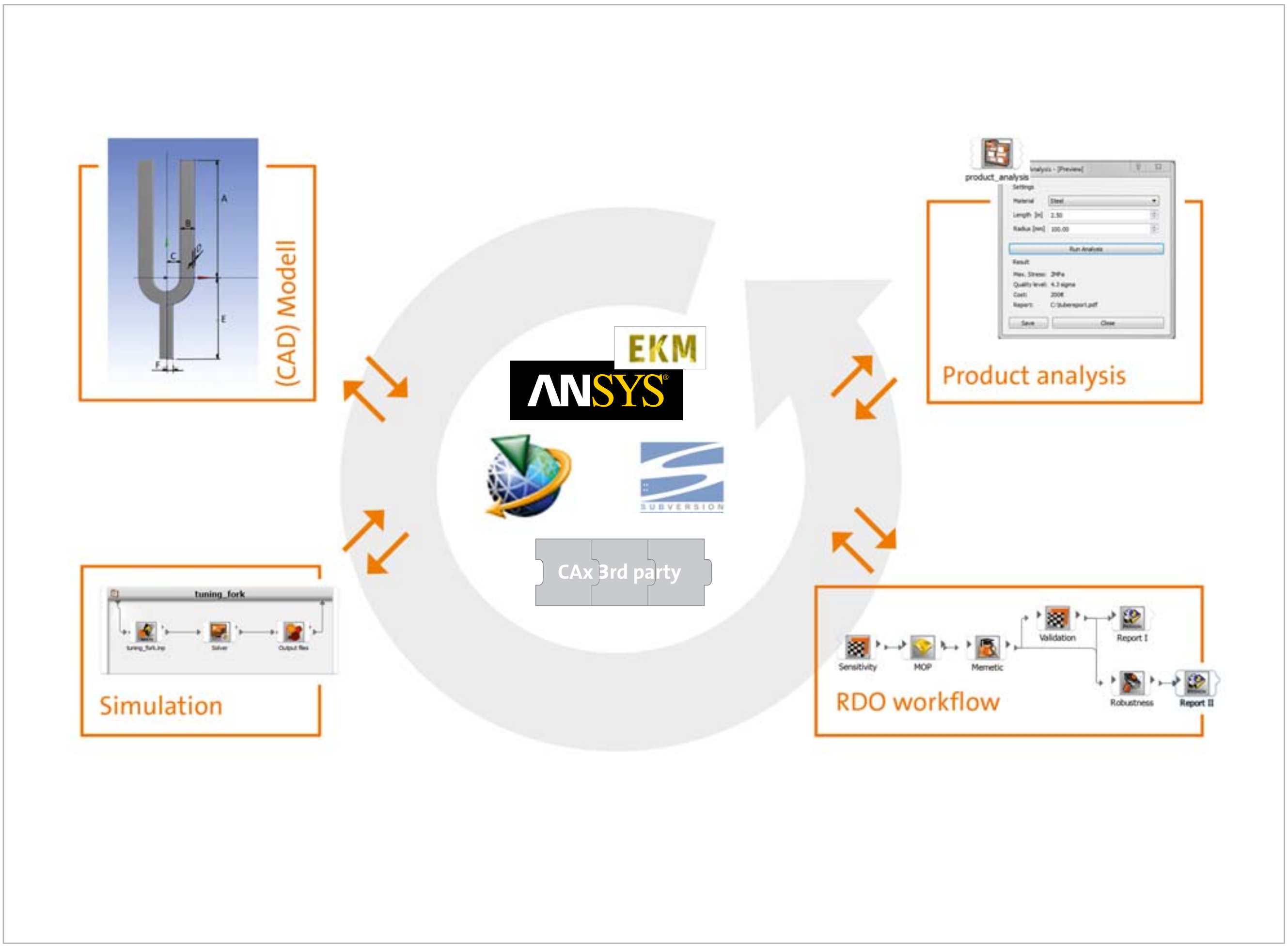

Fig. 2: Sceme of a modern Product Development Process using collaborative work based on a PLM / SPDM data base and optiSLang

Design of Experiments or Hardware Integration

In its truest sense, Design of Experiments (DoE) refers to evaluation of parameter value sweeps over a defined design space. DoE can be regulated manually or as an integrated Hardware-in-Loop (HiL) system. optiSLang could be used here as a data exchange interface tool to perform real-time sensitivity analysis and optimization on working systems. Together with Integrated Development Environment (IDEs) such as LabView, an automated measurement and result evaluation system could be set-up. Such an integrated system would prevent errors, minimize the total number of runs and hence provide immense savings in time and effort.

Such a HiL system was deployed by the Institute of Photonic Technology (IPHT, Jena) focusing on magnetometer characterization based on parameters such as laser frequency, source voltage, laser power and cell temperature and pressure. Manual characterization processes which took months for determining a single cell properties were replaced with an optiSLang + Engineering IDE system. This ensured optimal functionality, repeatability and optimization of the HiL system.

Further info: http://bit.ly/2bs9XEd

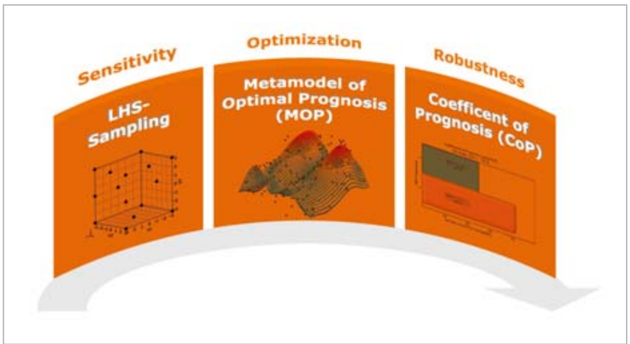

Fig. 3 : The statistical tools in optiSLang provide a good basis for Design understanding and design optimization.

Statistical post processing

Statistical analysis tools in optiSLang follow Dynardo's minimalist philosophy of allowing minimal user input with emphasis on ease-of-use and seamless integration functionality. Algorithms are designed and tested for robustness to cater noise or design zone failure within the paradigms of the design space. optiSLang automatically searches for the best possible correlation model in subdomains of important parameters with a given number of design points using the Metamodel of Optimal Prognosis (MOP®) workflow. That workflow becomes very powerful in large dimensions of input parameter and guarantees the user with the maximum amount of output information from given set of design points or experiments. Regardless of whether the raw data is acquired from Big Data analysis pool, Digital Twin or other resources, optiSLang offers efficient methods for Robust Design Optimization using sensitivity analysis, multidisciplinary optimization, parameter identification, robustness evaluation, etc. In terms of visualization and post processing, optiSLang provides diverse features such as illustration of nonlinear multidimensional correlation matrix, 2D and 3D anthill plots, meta-model forecast quality in terms of Coefficient of Prognosis (CoP®), Principal Component Analysis and illustration of statistical evaluations.

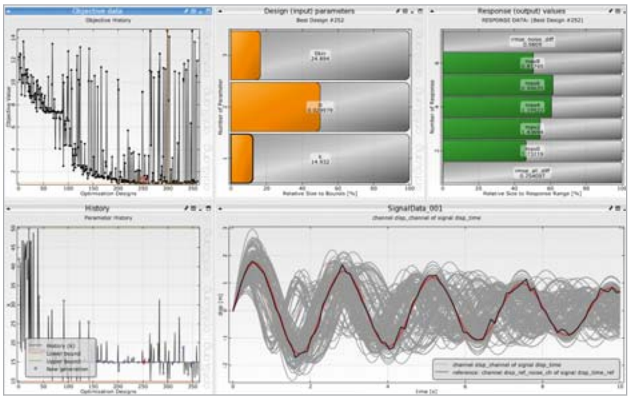

Fig. 4: optiSLang provides an enhanced visualization toolbox with histograms, signal channels and algorithm overview for design evaluation

Over the years, optiSLang's statistical algorithms have been employed across several backgrounds and domains. One such domain is Virtual Prototyping in the automotive industry.

In a joint study carried out at the Bergische Universität Wuppertal, optiSLang was used to generate a design space and carry out a Robust-Design Optimization of the machine element. The defined tolerances of the individual components were used to determine the design space and the normal stress distribution was extracted as a fitting response. It was illustrated that optiSLang could play a key role in Tolerance Management and meet the objectives of suitable, controllable and centered processes for the automotive industry.

Further info: http://bit.ly/2b9dlla

Databased ROM

Dynardo's concept of Databased ROM (DB-ROM), extends beyond the general definition of meta-data for concept evaluation. It is designed to be a critical component of the process

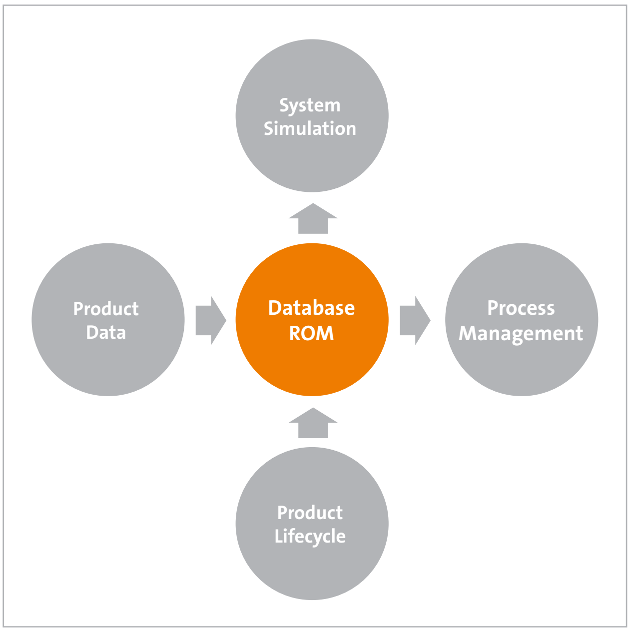

Fig. 5 : Databased ROM provides a crucial link to interfaces such as Digital Twin, System Design, Process Workflows and Product Lifecycle Management.

The vision of optiSLang's meta-model as a Databased-ROM hub is vividly illustrated with the automated optimization study of a machine tool cascade controller by CADFEM GmbH. The study uniquely highlights process abstraction, system simulation capabilities and integration into already created workflows using Simplorer.

Further info: http://bit.ly/2bwoUnp

server, acting as interfaces between several hubs of Product Development cycle. In this regard, Dynardo's DB-ROM can serve as a source of information using defined protocols between PLM systems, Big Data sources and participating CAx processes. It follows Dynardo's 'One-for-All' principle and is designed to be easy, safe, intuitive resource which can be easily retraced at various junctures of VPDP. Dynardo's DB-ROM is physics and environment independent and can function seamlessly in a co-simulation environment, as a monitor of IoT process. This allows the user to build a simulation-controlled Robust Design Development module where design robustness and optimization could be handled at the entry-point of virtual product development.

Virtual Product Development – CAx workflows, RDO, calibration and PLM

With the introduction of Lean Management in Product Development Processes, the role of CAx processes has become commonplace. Although hardware-based product tests form the core processes in a modern product development envi-

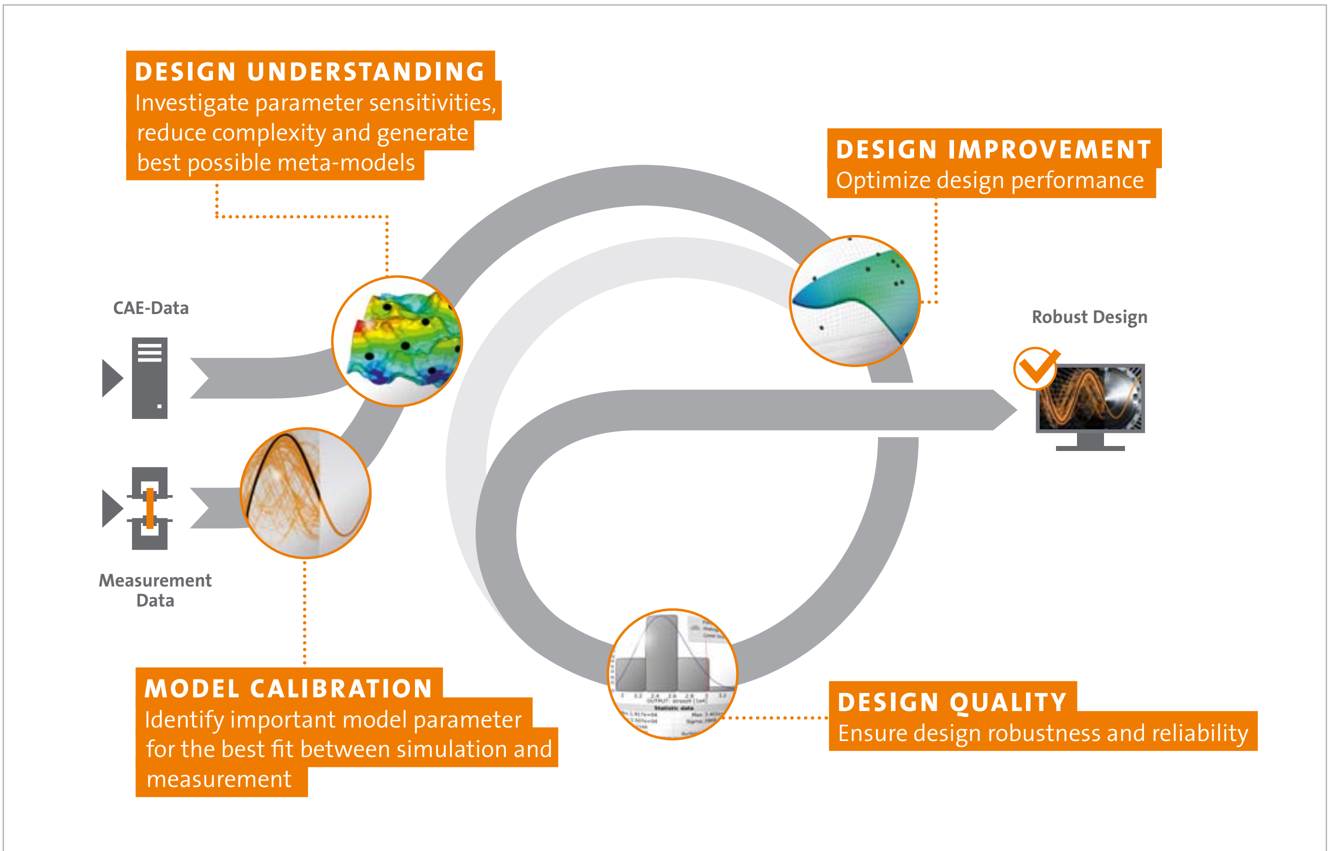

Fig. 6 : Dynardo's products support Virtual Product Development cycle through various gates and milestones in the PDP.

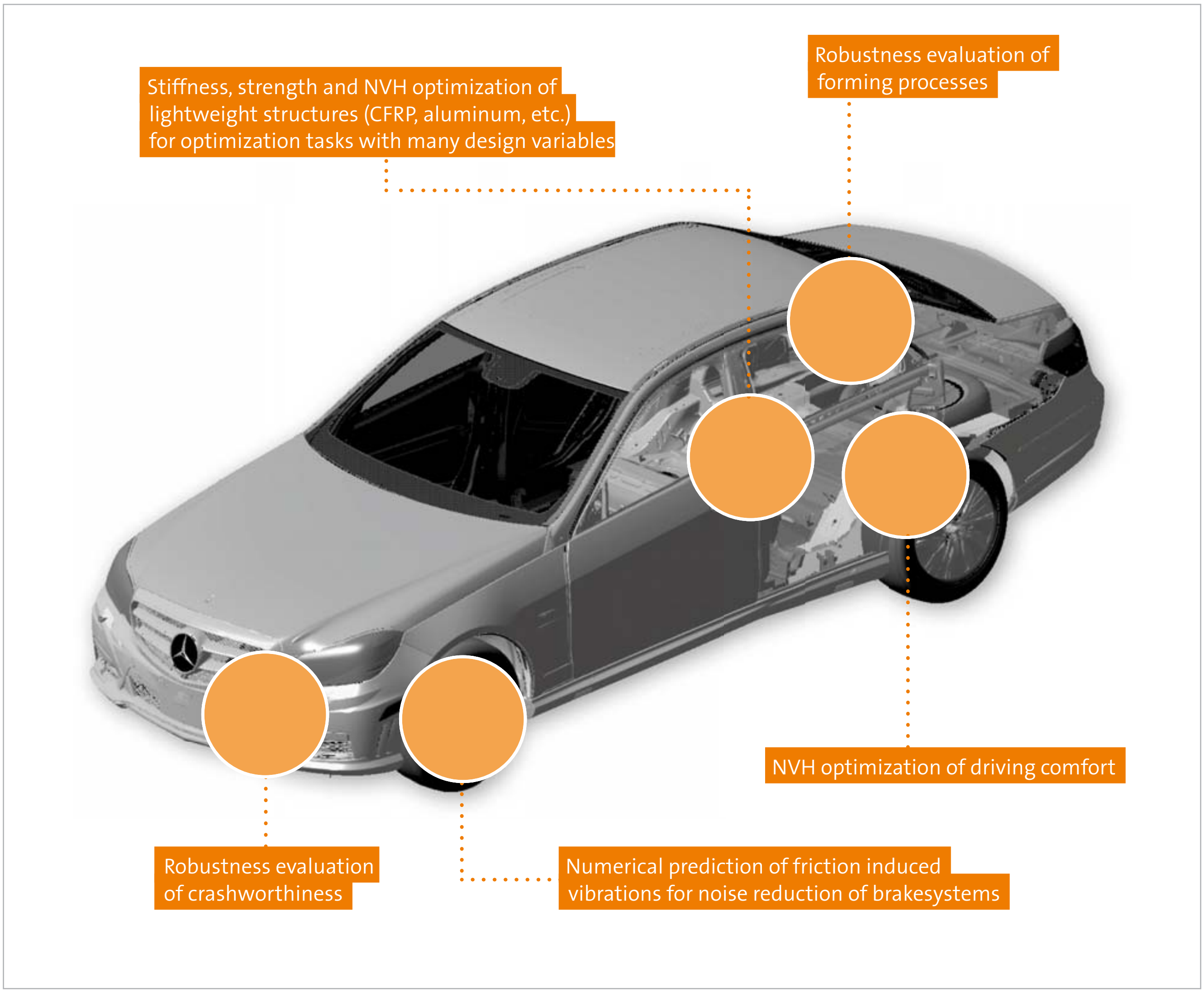

Fig. 7: optiSLang is being used to perform design optimization across the automotive sector (Courtesy Daimler AG)

ronment and simulation – based approaches still require real-world validation, the advent of robust CAE processes with high-end HPC systems has put numerical simulation at the forefront of PDPs. Herewith, Dynardo's 'One-for-All' philosophy extends beyond specific physical phenomena and bridges the gap between real and virtual world environment with integration modules for Hardware, PLM, VPDPs, etc. In this context, optiSLang provides an interface to bring various tools in VDP to a common platform and serve as an explicit parameter management system for process integration solutions.

The next generation of optiSLang provides direct access to the parametric modeling of CAE environments like ANSYS or SimulationX as well as to programming environments like EXCEL, MATLAB or Python. It allows users to combine several tools in sequences and iteration loops. As a control tool, optiSLang circumvents the errors associated with failed designs due to missing licenses, unfeasible geometries and other inconsistencies. optiSLang extends above and beyond a single OS-based platform, i.e. modules compatible with Windows, Linux and HPC as well as Cloud computing are provided. The following section gives an outlook of software application in the various phases of PDP:

1. Model Calibration

When Siemens AG attempted to estimate the pretension loss due to bolt temperature, optiSLang was chosen to perform FE-model calibration and subsequent Robust Design Optimization. Using optiSLang's Extraction Tool Kit (ETK), all post-processing results were gathered and the application of signal processing tools in optiSLang enabled the identification of calibrated FE-model parameters. Based on the calibrated model, a subsequent RDO was carried out to complete the optimized design process-chain. Additionally, optiSLang was identified as an efficient module to investigate robustness and optimization in the daily design process.

Further info here: http://bit.ly/2bzXexY

2. Automated CAx Workflows

Product Engineering at Robert Bosch GmbH and Daimler AG has seen optiSLang at the entry-point of VPD. As a driver of

CAx processes, optiSLang has been used to generate automated workflows to address the various phases of CAE modules and bridge interfaces between CAD-CAE-CAM hubs. Automation of CAE modules along with available HPC technologies has accelerated product development to new levels and with features such as FMU export, Excel add-in, SPDM extensions, optiSLang is leading the race for next generation process integration schemes. Moreover, custom integration options with 3rd party softwares such as Comsol, GT-Suite, NX, Simulation X has widened the scope of application of optiSLang across various domains and sectors.

Further info here: http://bit.ly/2cc7XML

3. Robust Design Development

Robust Design Optimization with optiSLang is based on 'minimum input – effective development' philosophy. The goal of CAE-based optimization in virtual prototyping is often to achieve an optimal product performance with a minimal usage of resources (e.g. material, energy). This pushes designs to the boundaries of tolerable stresses, deformations or other critical responses. Conducting a sensitivity analysis, multidisciplinary optimization, robustness evaluation and reliability analysis with optiSLang enables the user to quantify risks, identify optimization potential, improve product performance, secure resource-efficiency, save time to market, etc. The Robust Design Optimization (RDO) combines CAE-based optimization with robustness evaluation and allows a product optimization with a synchronized assurance of robustness. A classica example involves our customer story from Daimler AG with the analysis of shape accuracy of single and assembled parts. A process-workflow was created to simulate a S-rail forming and joining process-chain to analyze the sensitivity of the model parameters. As a result of the investigation and the use of meta-models for sensitivity analysis, the calculation time for RDO of forming and forming station parameters were reduced and the translation effects of S-rail plates could be better understood.

Further info here: http://bit.ly/2bncGP4

4. PLM Integration

Integration of DB-ROM or CAx database into PLM systems still remains a challenge since interfaces with multiple software support are not yet supported. However, optiSLang provides a feasible solution to create parametric process workflows with automatic integration to PLM systems such as ANSYS EKM, Siemens Teamcenter, etc. At the same time, optiSLang allows for seamless integration into existing process workflows. So whether it is transfer of data between Big Data Analytics and CAx processes or the assimilation of VPDP within the complete manufacturing cycle, optiSLang provides a one-stop solution for access to and from PLM systems.

Further info here: http://bit.ly/2cT31Os

Conclusion

The new generation of optiSLang has moved beyond the conventional general purpose tool for variation analysis. All in all, optiSLang provides solutions to challenges prevalent in each phase of PDP. With its modular nature, the software can be moulded or upgraded based on industry's needs. With newer and other user-customizable features already on the roadmap, optiSLang is showing great promise to become a powerful bridge between next generation CAx (CAD, CAM, CAE) processes.

The key points, in view of a successful Product Development process, can be highlighted under the following:

- Automation and Standardization of VPDP workflows
- Parametric studies and Robust Design Optimization
- Flexibility and Extensibility
- Supporting continuous improvement
- Enabling collaborative work

Authors //
Animesh Ranjan, David Schneider (Dynardo GmbH)

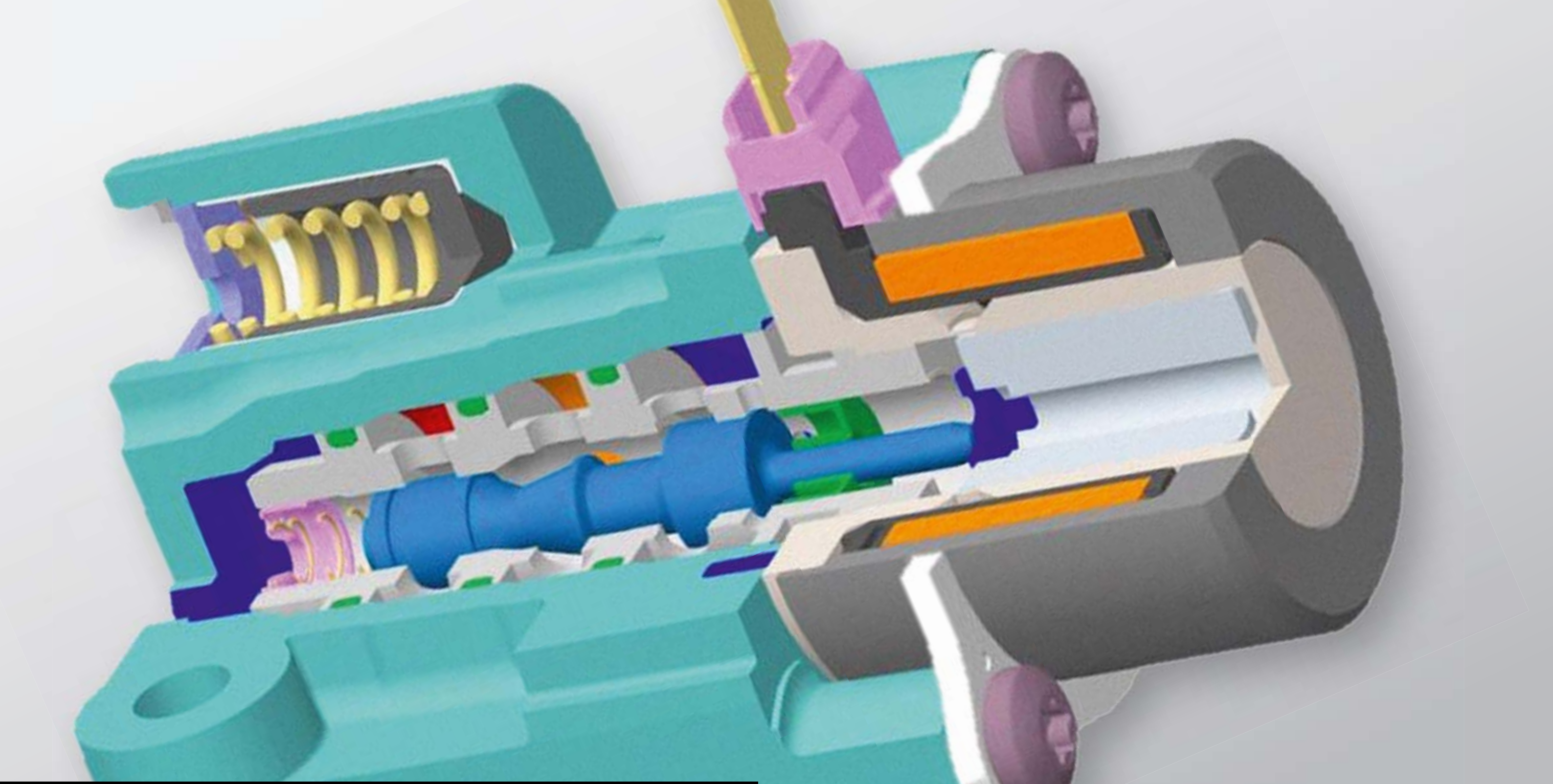

CUSTOMER STORY // MECHANICAL ENGINEERING

OPTIMIZATION OF A PISTON GEOMETRY IN A PRESSURE CONTROL VALVE

optiSLang supports the optimization of a piston geometry to improve the response time of the valve and the flow rate.

Task Description

The problem to be solved deals with a 3/2 proportional pressure control valve of a DCT transmission which regulates the filling of the clutch due to the valve. Inside the valve, a bucking occurs in certain situations during shift operations. Therefore, response times have to be improved in order to ensure a fast filling of the clutch. Better response times ought to be achieved by reducing the flow forces in the valve.

Fig. 1 shows the function of the valve as part of the clutch mechanism. As soon as the piston moves and the valve opens, oil flows from the P-port to the A-port finally filling the clutch. During this operation, opposite loads occur to the magnetic force, which moves the piston. Due to high loads, especially high pressures at small openings, the valve does not operate as fast as desired.

The operating speed of the valve is recorded as the response time. Fig. 2 shows the distribution of this period and its classification in the pressure curve. The time between the response of the valve and the first reaction of the pressure is called "dead time". The duration of reaching 90 percent of the target pressure is called "filling time". By reducing the

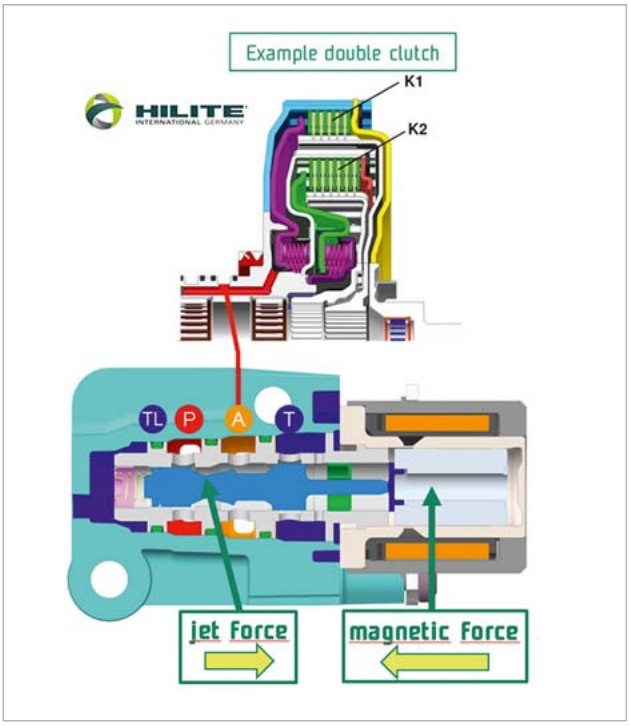

Fig. 1: Functional scheme of the pressure control valve in the clutch

flow force, the magnetic force causes more effect on the piston resulting in a faster response. This mainly affects the period of filling and leads to a lower overall response duration. At the same time and in addition to the flow force, the flow rate has to be monitored for keeping it as high as possible in order to ensure a quick filling of the clutch through the valve.

Simulation and optimization

The flow optimization of the piston inside the pressure control valve is performed with optiSLang and ANSYS CFX. optiSLang determines the piston designs to be calculated, evaluates the results of the simulation and identifies new designs based on these results. The calculation of the flow force and the flow rate on the piston is conducted by ANSYS CFX. The calculated data is then transferred to optiSLang.

For the optimization, a model adapted to flow calculation is used. Here, all important geometry parameters can be varied. The model and the corresponding geometry parameters are displayed in Fig. 3. A range of acceptable variations is set for each parameter. Certain parameters, such as the initial pressure P, are not changed but set to a constant value of 20 bar.

The CFX model shown in Fig. 3 represents the space in which the fluid flows from the P- port to the A-port. On one side, it

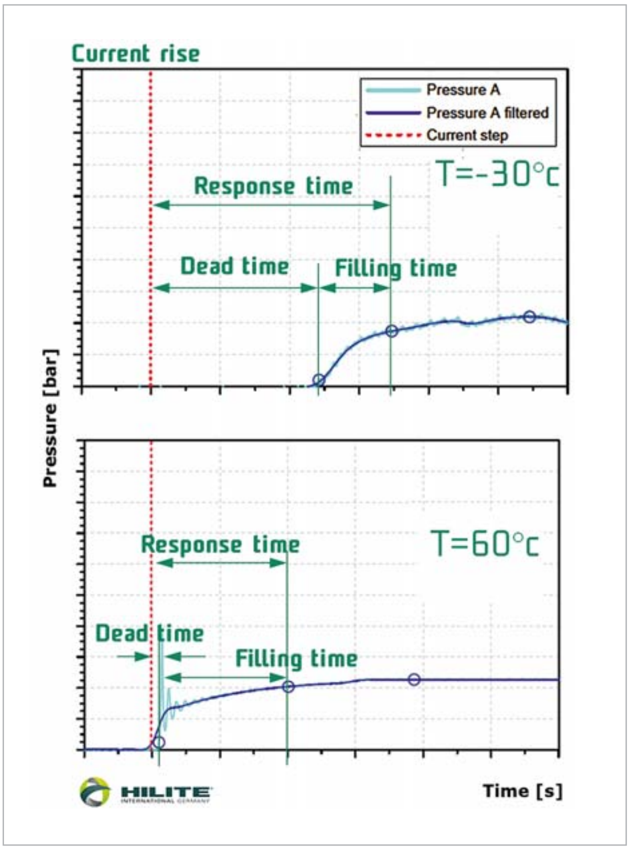

Fig. 2: Activation of the clutch in the gearbox with pressure regulating valve - low temperature (top) - normal temperature (bottom)

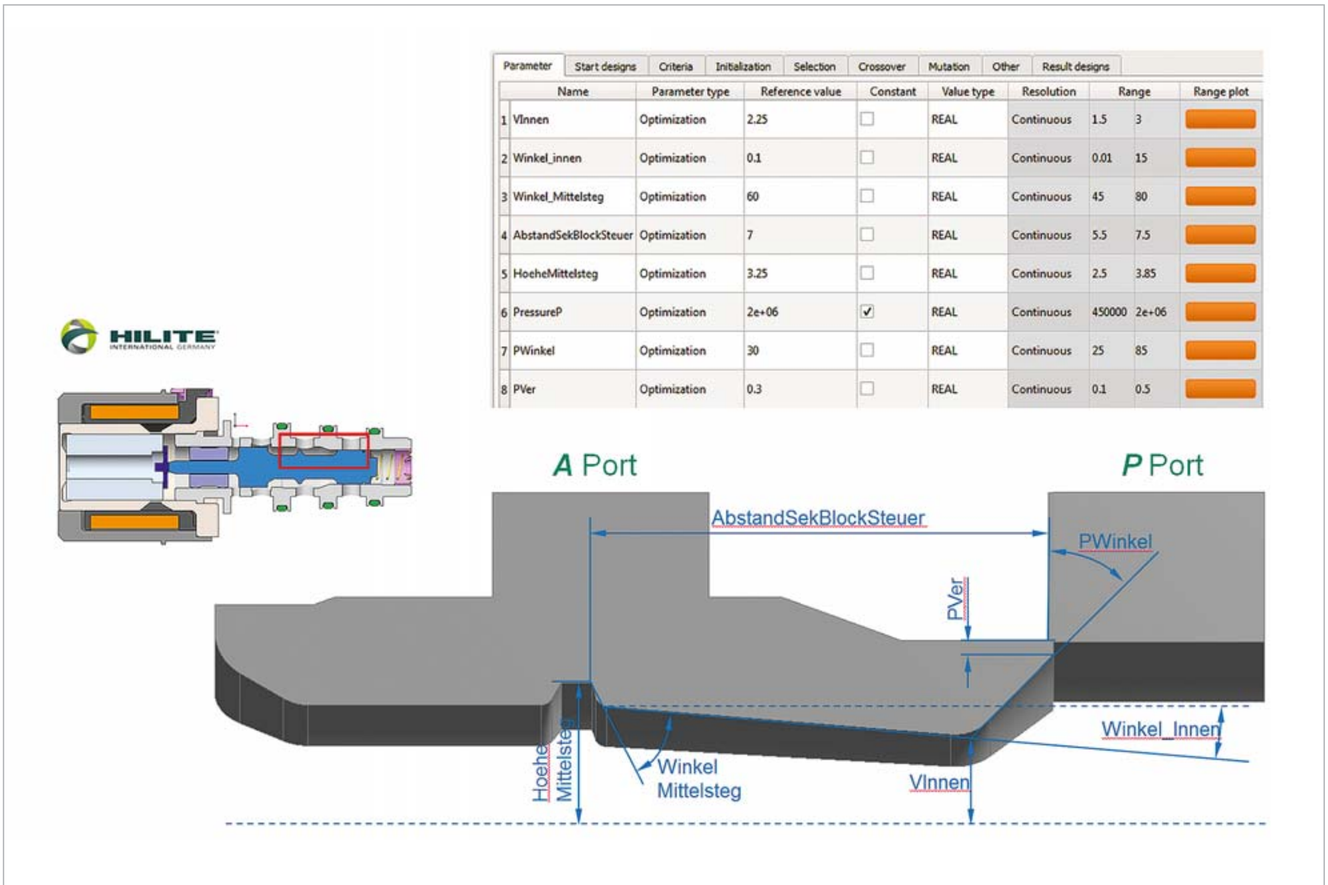

	Name	Parameter type	Reference value	Constant	Value type	Resolution	Range		Range plot
1	VInnen	Optimization	2.25	☐	REAL	Continuous	1.5	3	
2	Winkel_innen	Optimization	0.1	☐	REAL	Continuous	0.01	15	
3	Winkel_Mittelsteg	Optimization	60	☐	REAL	Continuous	45	80	
4	AbstandSekBlockSteuer	Optimization	7	☐	REAL	Continuous	5.5	7.5	
5	HoeheMittelsteg	Optimization	3.25	☐	REAL	Continuous	2.5	3.85	
6	PressureP	Optimization	2e+06	☑	REAL	Continuous	450000	2e+06	
7	PWinkel	Optimization	30	☐	REAL	Continuous	25	85	
8	PVer	Optimization	0.3	☐	REAL	Continuous	0.1	0.5	

Fig.3: Input of geometry parameters in optiSLang (top), variable geometry parameters of the piston model in CFX based on a sample design with an opening of 0.1mm (bottom)

is bounded by the inner surface of the bushing and, on the other side, by the external geometry of the piston. If the geometry of this "negative volume" is varied, the form of the bushing or piston is also automatically changed.

There is a critical range at high pressure and small openings of the valve where the flow force has to be reduced. Thus, for the optimization, the maximum pressure of 20 bar should be initiated at the A-port and the flow forces should mainly be calculated at low openings. For each geometry generated by the optimizer, the flow force and the flow rate on stroke positions (opening at the P-port) 0.025 mm, 0.05 mm, 0.15 mm and 0.4 mm is calculated.

Here, the optimization goals are the reduction of the flow force on the piston and the increase of the flow rate. To pursue these two objectives simultaneously, an evolutionary algorithm is used, which seeks Pareto optimal solutions.

As Fig. 4 shows, only the three smallest response parameters are used for the objective of reducing the flow force (Obj_ForceMIN). The opening of 0.4 mm serves as a control parameter (constraint) ensuring the optimized design to be more efficient than the reference even at large openings.

For reaching the objective of maximizing the flow rate (Obj_FlowMAX), the results of all four stroke parameters are used. For an improved optimization potential, the flow rates are weighted differently in order to obtain homogeneous individual values. In the case of achieving both optimization objectives, the valve should respond and operate at a significantly improved response time, with the clutch to be filled faster and the problem of bucking to be solved. Additional constraints, which are not shown here, ensure the calculation of only solvable geometries. Invalid geometry combinations are sorted out beforehand.

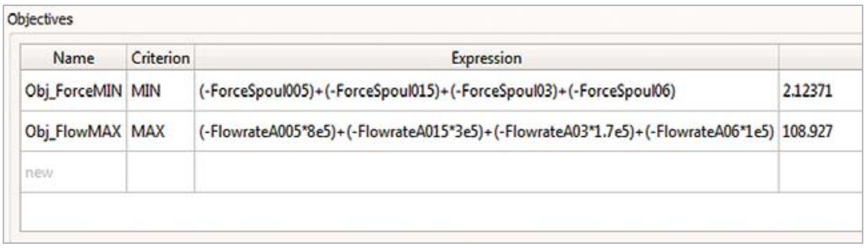
Objectives

Name	Criterion	Expression	
Obj_ForceMIN	MIN	(-ForceSpoul005)+(-ForceSpoul015)+(-ForceSpoul03)+(-ForceSpoul06)	2.12371
Obj_FlowMAX	MAX	(-FlowrateA005*8e5)+(-FlowrateA015*3e5)+(-FlowrateA03*1.7e5)+(-FlowrateA06*1e5)	108.927
new			

Fig. 4: Definition of optimization goals (objectives) in optiSLang

Fig. 5: CoP matrix of the sensitivity analysis regarding the CFX examination of the pressure control valve

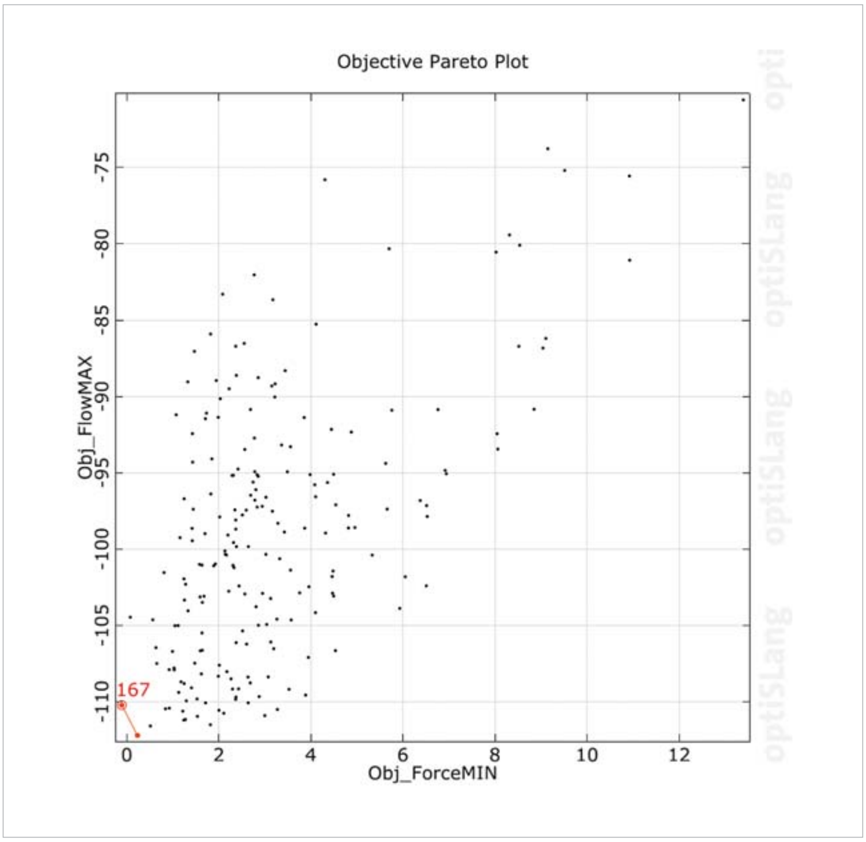

Fig. 6: Pareto plot of the piston VKP designs in the sensitivity analysis

To limit the optimization space and to be able to identify potentially relevant parameters in advance, a sensitivity analysis is performed before the actual optimization. In this case of flow optimization, the analysis includes approximately 200 designs covering the parameter space of the seven variable geometry parameters. The computational time of one design takes about 20 to 30 minutes.

Because the objectives for the optimization have already been integrated in the sensitivity analysis, the results can be analyzed and used as starting values for the optimization. Thus, computing time is saved and optimal geometries can be found faster if the result space is limited before. In the subsequent optimization of the piston, another 70 designs are calculated to find the optimal design.

Results of the piston flow optimization

Sensitivity analysis of the pressure control valve piston
The sensitivity analysis provides an overview of the influence of geometric variations of the flow rate and flow force on the piston (ForceSpoul) regarding the objective functions. In contrast to the optimization, different values of valve openings, here 0.05 mm and 0.15 mm for small openings and 0.3 mm and 0.6 mm for large openings, are used to cover the entire opening range as much as possible.

The only parameter in the predefined range of variation having no impact in the analysis is the angle at the center bar. The height at the center bar is particularly sensitive with larger openings regarding both goals “ForceSpoul” and “FlowrateA”. The same behavior can be observed during the variation of the distance between the central bar and P-port (“AbstandSekBlockSteuer”).

The angle at the P-port (“PWinkel”) and the height of the edge of the P-port (“PVer”) mainly affects the flow rate. In addition, there is also an effect on the flow force with small openings.

The variation of the inner radius of the piston (“Vinnen”) particularly influences the flow force at small openings. The corresponding angle (“Winkel_Innen”) also changes the flow force, but this is only significant at an opening of 0.15 mm to 0.3 mm.

Already during the sensitivity analysis, the optimization goals have been implemented in optiSLang. Therefore, the calculated designs can be analyzed accordingly. Fig. 6 shows the resulting Pareto plot, in which all geometries calculated in the sensitivity study are evaluated regarding the corresponding values of the objective functions. Here, the clear trend can be seen that certain geometries are distinguished by a particularly low force and a high flow rate. Those designs with the best inclusion of both objectives are marked as Pareto optimal (red dots) and are located in the lower left corner.

They are used as starting parameters for a subsequent optimization. Thus, the algorithm already starts in a pre-located space and can find the optimal piston geometry more easily and quickly.

Flow optimization of the pressure control valve piston
Due to the two optimization goals and the sufficient start designs, after 70 designs, i.e. the 5th generation after the starting design, an optimal piston geometry could be found. The three designs DP08, DP43 and DP48 fulfill all constraints and are characterized by a reduced flow force. Fig. 7 shows the optimized design accordingly organized to their quality of results. In the left lower corner, the top three variants are marked in red. Each of the three geometry variants has its pros and cons.

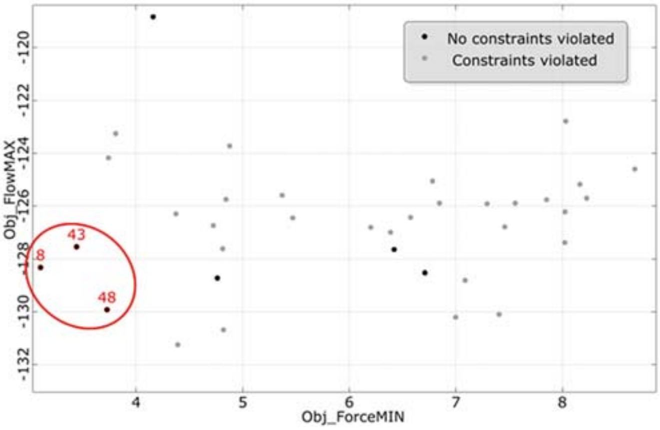

Fig. 7: Result of the optimization with evolutionary algorithms - optimal designs marked in red

Design Point 08 (DP08) is characterized by the lowest flow force (Obj_ForceMIN), but shows an unfavorable force curve and no optimum flow at the maximum opening.
DP48 shows the largest flow rate (Obj_FlowMAX) at the maximum opening and is characterized by a very uniform force curve. However, this design causes the highest flow force in comparison to the others.
DP43 is characterized by low flow forces especially at very small openings. Furthermore, the force characteristic is very balanced like DP48, but shows a lower flow force. The disadvantage of this piston geometry is the low flow rate.

The optimization results of the three selected piston geometries can be seen in Fig. 8 and 9 (see next page). Due to the favorable characteristics and the low flow forces, design number 43 is considered to be the most suitable piston geometry.

Compared to the reference valve, the resulting changes in the optimal design are particularly visible in Table 1. The biggest adjustments can be seen in the range of the two angles

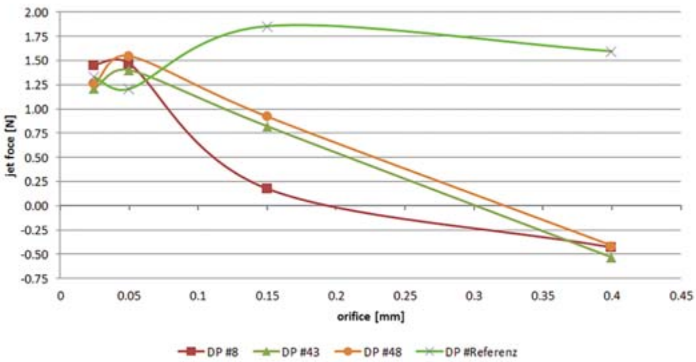

Fig.8: Results of the calculated flow force in the ANSYS CFX Designs DP08, DP43 and DP48 (jet force plot of optimal designs)

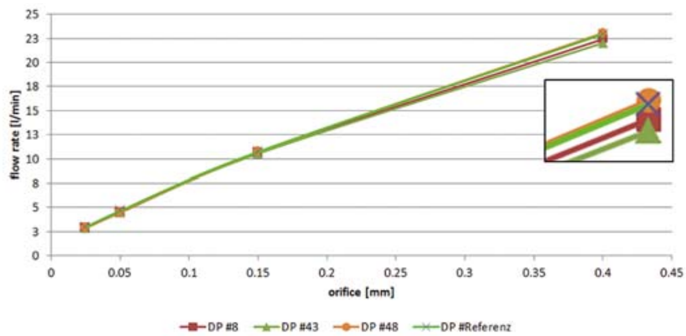

Fig. 9: Results of the calculated flow rate rate in the ANSYS CFX Designs DP08, DP43 and DP48 (flow rate plot of optimal designs)

"PWinkel" and "Winkel_Innen". Other major changes are made in the parameters "AbstandSekBlockSteuer" and "Vinnen". The result of the changes can be seen by comparing the piston geometries in Fig. 10. The geometry of the reference design is depicted at the top and the optimized design at the bottom. The interaction of the parameters results in a significant change of the piston geometry. The former straight graph (Fig. 10, top) now shows a "V-shape" (Fig. 10, bottom). By the aerodynamically favorable shape, the force is reduced over the entire opening range and causes a balanced force characteristic. However, depending on the entrance angle of the flow, the forces on the piston are also changing in this geometry. This becomes very clear when looking at the flow force curve. Fig. 11 and Fig. 12 represent an accurate recalculation of the force and flow characteristics over the entire range of valve openings for the reference and the optimized piston. The flow forces affecting the piston during the opening are depicted blue in the optimized geometry, the forces of the reference geometry are marked in red. Depending on the applied pressure, the characteristics become darker. Pressures of 5 bar, 10 bar and 20 bar are shown.

The optimization aims at the reduction of the flow forces, especially at low openings. Unfortunately, this goal could not be reached entirely in the optimization. For very small openings, only slightly smaller forces could be achieved.

ID	Distance Sek BlockSteuer	Hight center bar	PVer	PWinkel	VInnen	Angle center bar	Angle inner
Reference	7.00mm	3.25mm	0.300mm	30.0°	2.25mm	60.0°	0.0°
Optimized Design DP43	6.63mm	3.20mm	0.397mm	66.4°	1.837mm	76.7°	12.7°

Table 1: Geometry parameters of the reference and the optimization of the pressure regulating valve piston

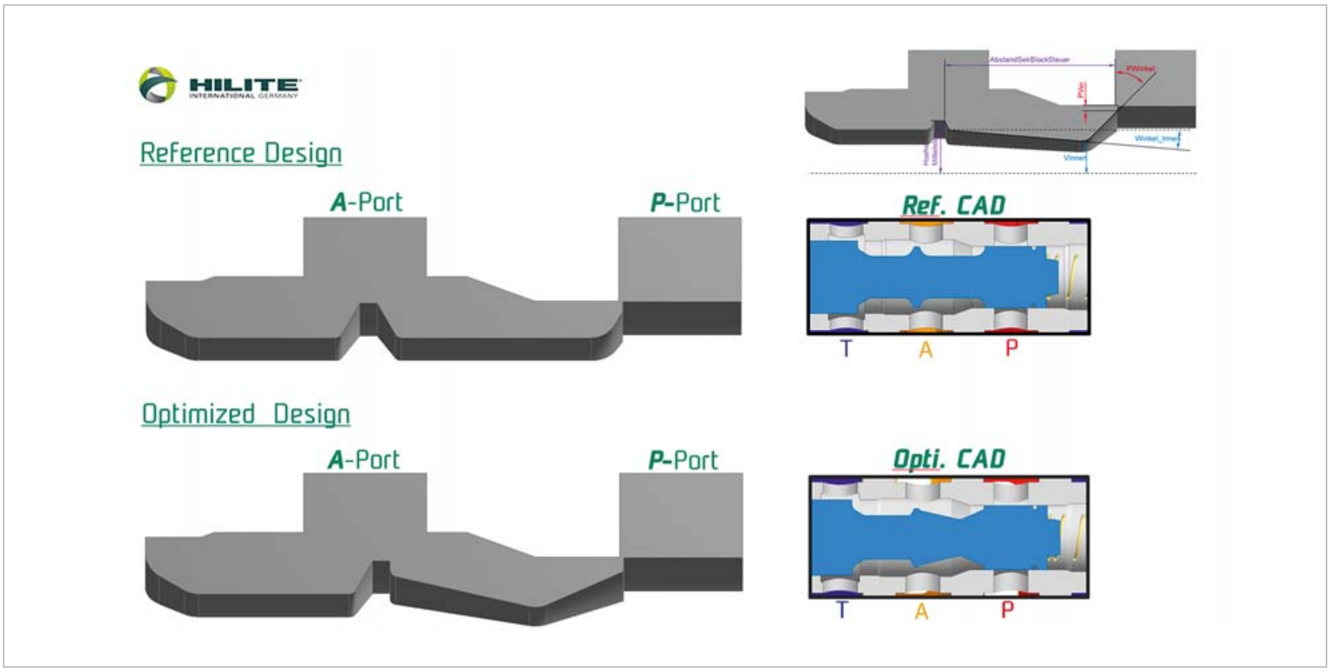

Fig. 10: Reference geometry (top) and optimized geometry (bottom) of the VKP piston at 0.4mm opening

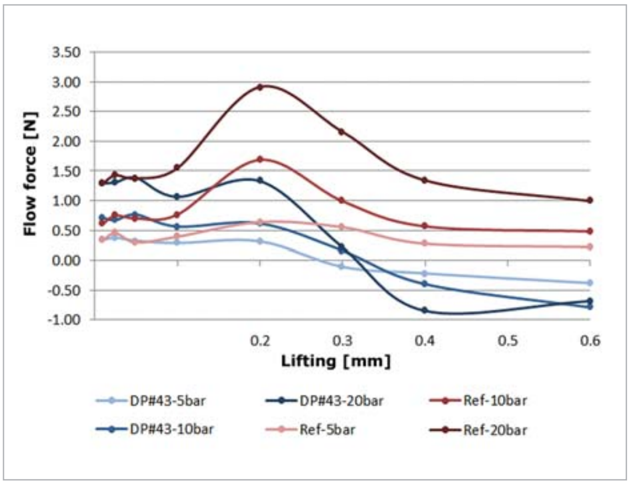

Fig. 11: Comparison of the course of flow force on the VKP piston for the reference (red) and the optimized (blue) Design

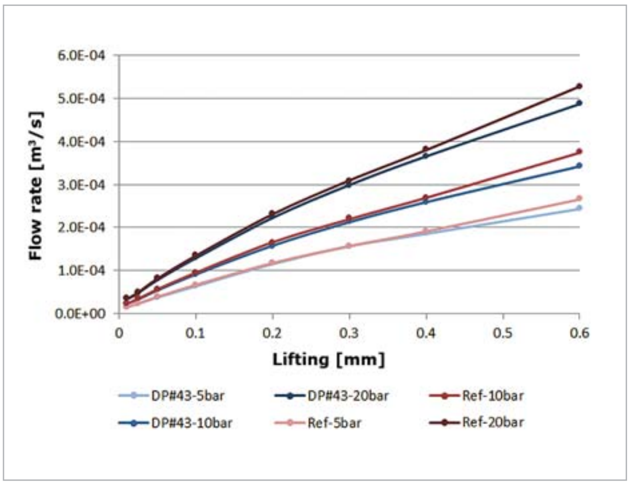

Fig. 12: Comparison between courses of the flow rate in the VKP - reference (red) and optimized (blue) Design

If the valve is opened wider and, thus, conveying more fluid, the advantage of the new geometry becomes obvious. The reference design shows an increase in the flow force from 0.1 mm opening, whereas the optimized design reduces the affecting flow force on the piston. The maximum applied flow force is reduced according to the pressure by up to 50%. Due to the new geometry, not only the amount of the maximum applied force changes, but also its occurrence being now at a smaller opening.

Up to about 0.4 mm opening, the flow force counteracts the magnetic force. If this point is exceeded, the closing flow force on the piston turns into an opening one supporting the magnetic force.

Although an optimization goal for improving the flow rate has also been defined, it is not possible to combine the reduction of the flow force with an increase of flow rate. The initially small differences between the reference and DP43 are constantly increasing with a wider opening. The maximum reduction of the flow rate of 7% is only reached at the maximum opening of 0.6 mm. Since this position is relatively rare in operation, the difference from the reference is usually less than 7%.

The pressure curve, which is plotted in the left section of Fig. 13, is similar in both piston variants. In this case, there are differences between the positions of the pressure concentration. The pressure reduction is concentrated in the opening range at the P-port of the optimized variant showing a balanced characteristic. At the top of the "V-shape", an additional high pressure zone can be seen because, here, the flow is diverted in a different direction.

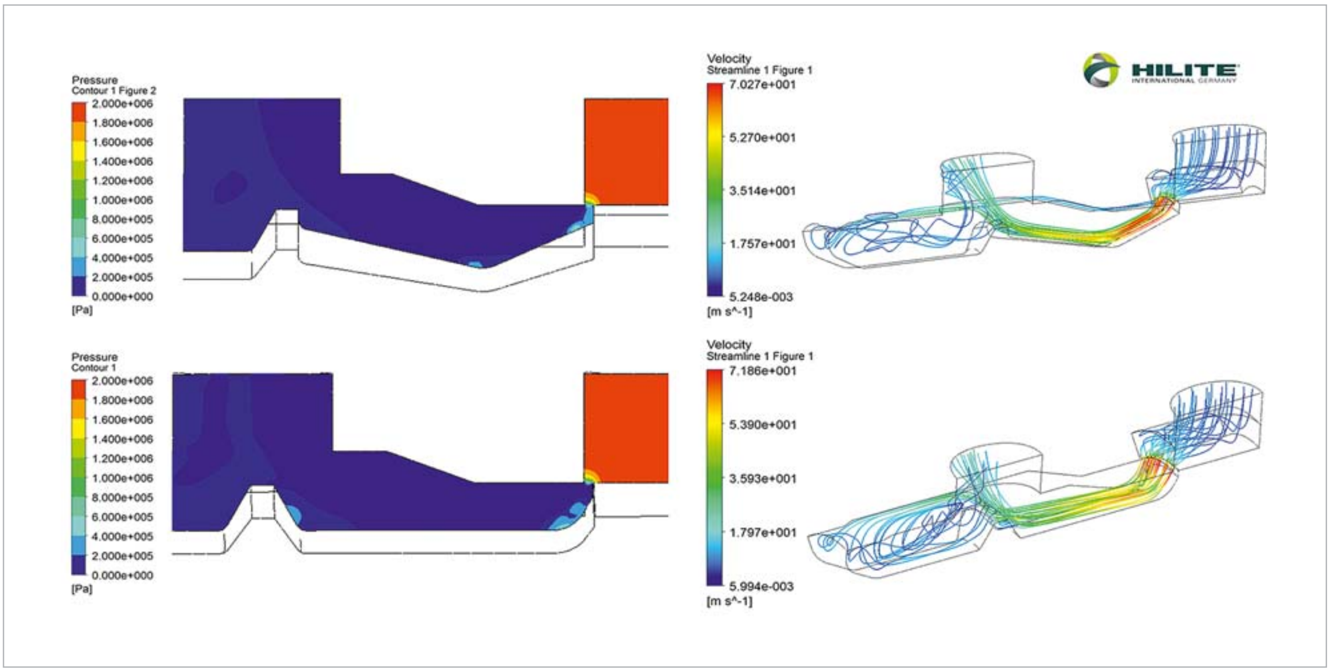

Fig. 13: Comparison of the pressure and the velocity of the VKP for the reference and the optimized piston

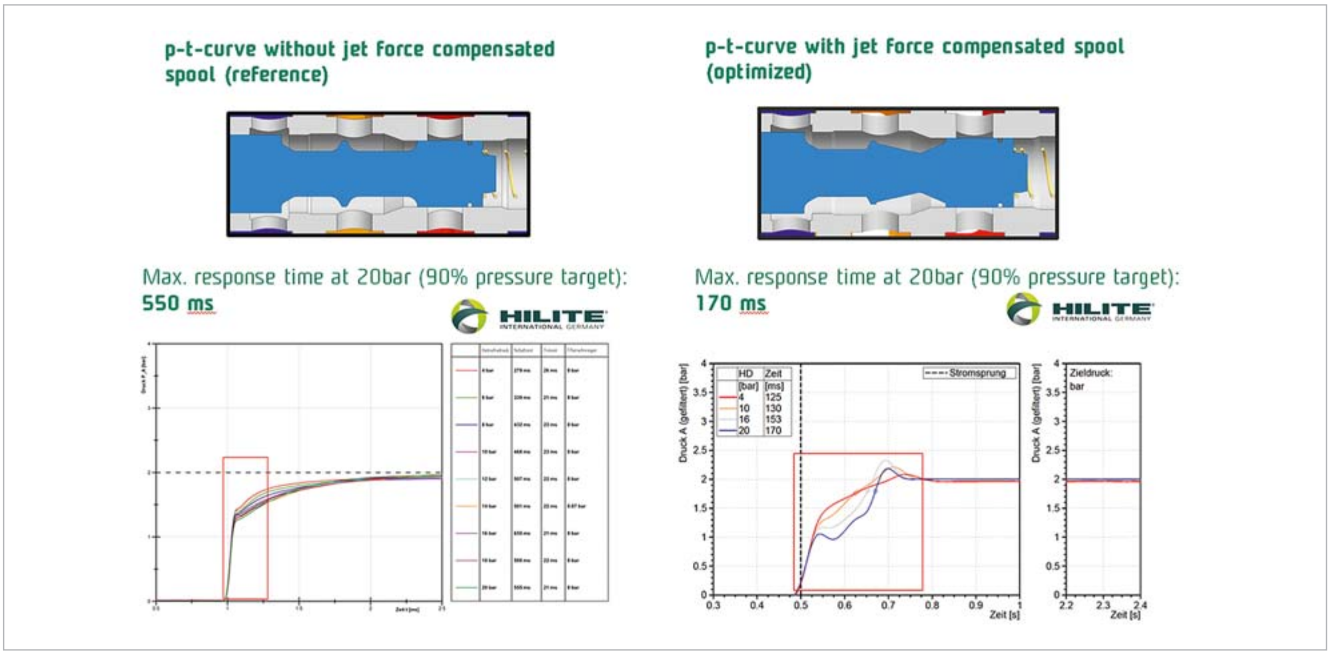

Fig.14: Comparison of the p-t curve with and without flow-compensated piston

The velocity profile of both pistons is shown in the right section of Fig. 13 (see previous page). Here, the flow on the optimized piston shows a larger and longer lasting speed due to the improved shape. The fluid is not slowed down too fast, which is clearly indicated by the longer red areas of the speed curves.

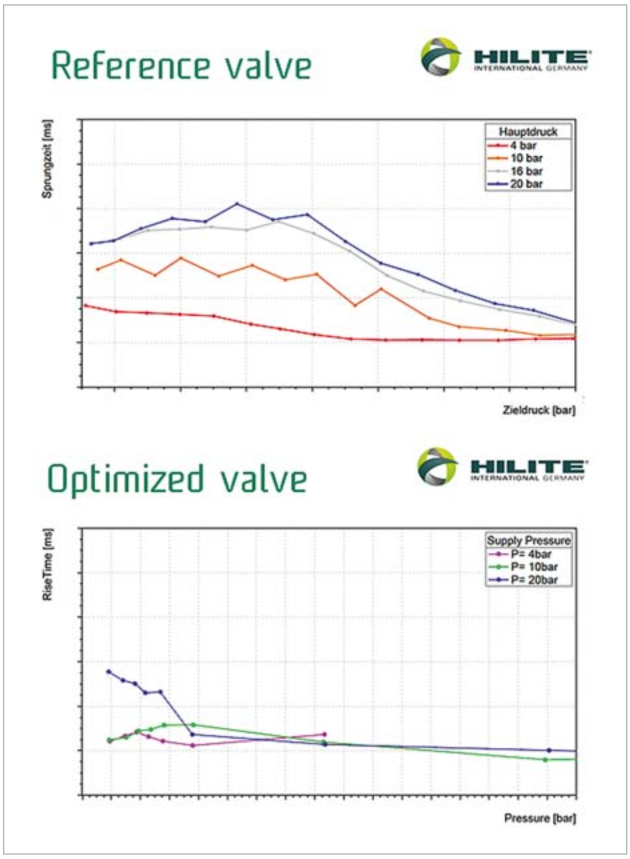

Fig. 15: Comparison of the skip times of the pressure control valve with and without flow-compensated piston

For the calibration of the simulation, prototypes of the valve with the optimized piston are tested. It turned out that the flow compensated piston of the pressure control valve also obtained a significant improvement in the experiment. The response time in Fig. 14 as well as the jump times in Fig. 15 show the gain in speed as a result of the optimization.

The p-t curves shown in Fig. 15 indicate the measured filling time of the optimized and non-optimized valve at different pressure jumps. 90 percent of the pressure jump of 20 bar is achieved with the valve of the standard piston in 550 ms. When the optimized variant is used, the time is reduced by almost 70 percent to 170 ms.

Regarding the jump time, Fig. 15 shows a similar picture. The maximum jump time (maximum step response) at 20 bar supply pressure is reduced by 1/3 from 420 ms with the standard piston to 280 ms using the flow-compensated piston.

The pressure dependence is located within a range of less than 200 ms and, thus, was reduced by 50 ms to 100 ms.

By the optimization using optiSLang and ANSYS CFX, a piston design could be found where the objectives are considered and the optimization eliminates the problems successfully. The expected improvement is confirmed both in tests and in vehicle prototyping. The problem of bucking during vehicle operation is solved.

Author // Christian Hugel (Hilite International GmbH)
Source // www.dynardo.de/en/library

WELCOME TO THE

WOST

ANNUAL WEIMAR OPTIMIZATION AND STOCHASTIC DAYS

Your conference for CAE-based parametric optimization, stochastic analysis and Robust Design Optimization in virtual product development.

The annual conference aims at promoting successful applications of parametric optimization and CAE-based stochastic analysis in virtual product design. The conference offers focused information and training in practical seminars and interdisciplinary lectures. Users can talk about their experiences in parametric optimization, service providers present their new developments and scientific research institutions inform about state-of-the-art RDO methodology.

Take the opportunity to obtain and exchange knowledge with recognized experts from science and industry.

You will find more information and current dates at: **www.dynardo.de/en/wosd**.

We are looking forward to welcoming you to the next Weimar Optimization and Stochastic Days.

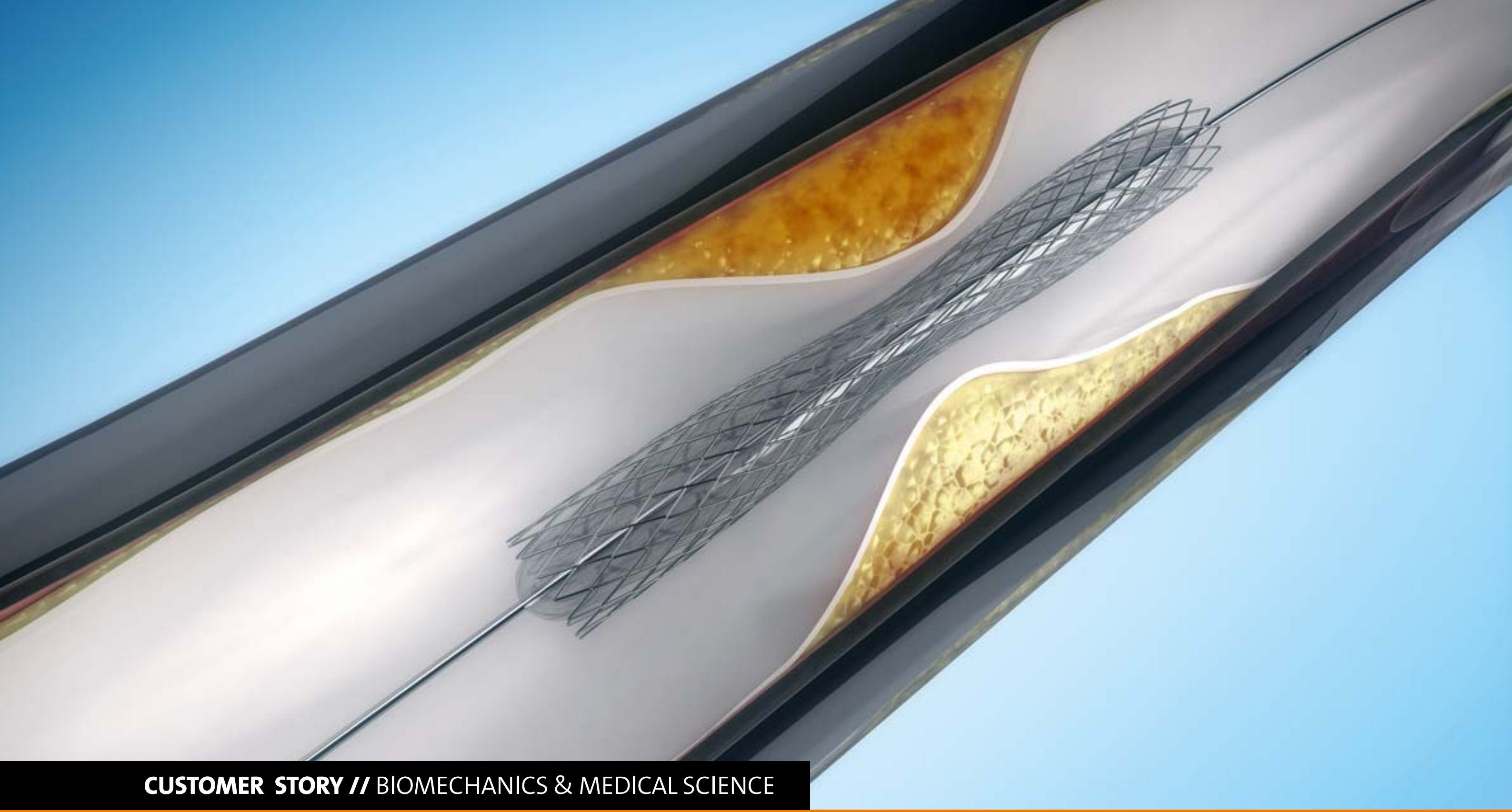

SIMPLIFIED METHOD TO PREDICT STRUCTURAL PROPERTIES OF CARDIOVASCULAR STENTS

ANSYS Workbench connected with optiSLang enables an analytical approach based on Design of Experiments (DOE) and statistical modelling in order to predict the radial force and strain amplitude of a circular stent structure.

Introduction

Vascular stents are used to treat occluded or calcified vessels or carry heart valve tissue in case of Transcatheter Aortic Valve Replacements (TAVI). The TAVI procedure was successfully introduced during the last decade and provides a safe option for elderly patients who are not suitable for conventional open heart surgery.

For all applications it is necessary in the design phase to predict the radial force and fatigue behavior of such devices. The radial force is a crucial parameter in preventing migration or even a collapse of the device under physiologic loading (pressure difference) or during the delivery (bending, crush). Similarly, the strain amplitude within a stent serves as an essential parameter for estimating the fatigue resistance of Nitinol stents.

In the medical device industry it is common practice to perform multiple design loops (CAD and FEA) to achieve a final design with preferable attributes. This process is time consuming and requires repeated interaction of the developer with multiple software tools. For all iterations a fully processed FEA model has to be calculated and evaluated which consumes time and physical resources. Therefore the present study aims to simplify this process by employing a Design of Experiments and statistical modelling.

Method

A fully parametrized CAD (Solid Edge) model of a single Nitinol strut which can be used in all closed cell stent designs was developed (Fig. 1). This model was imported into Ansys Workbench and connected with the optiSLang interface (Fig. 2). The main design parameters (strut length, radius and strut width) were included in a Design of Experiments (75 designs, Latin Hypercube Method) using the software optiSLang 4.1.2. As output parameters, the radial force and the strain amplitude within the clinically used design range were evaluated. Subsequently, the radial force for a complete circular stent structure was reconstructed based on a single cell. For all design iterations, the cell was shaped (heat treatment), crimped and deployed into a vessel followed by a radial force measurement and a cyclic cardiac pulse (pressure related decrease and increase in diameter). As a result, the radial force for the loading and unloading plateau (characteristic of Nitinol) was evaluated at the two extreme clinical diameters. Based on the 75 design points, a linear regression model was developed for all result parameters (radial force, strain amplitude) including all input variables (Software Minitab 17.0). The derived equations were then used to develop a simplified analytical prediction of the radial force and strain amplitude for a complete circular stent segment.

Fig. 1: Single diamond cell and the reconstruction of a 360° full stent model with 12 single cells

Results and discussion

A good agreement between experimentally measured and numerically simulated radial force was achieved for the exemplified stent design (Fig. 3, see next page). By summarizing the radial force of single cells and using an analytical equation, the radial force of a complete stent segment could be determined and validated by experimental data.

The evaluation points of the Nitinol curve are shown on the right. The table at the bottom shows the comparison of experimental vs numerical (FEA) and experimental vs statistical (analytical) model.

This allows estimating the radial force and strain amplitude of a complete circular stent segment by using a simple regression equation (equation 1 and 2; my_fsum3=radial force; ampl=strain amplitude DS_SL=strut length; DS_SBK=strut width at the radius; SBM=strut width in the middle). In the preliminary design phase during the product development, this procedure holds the potential to save computational time and accelerate the design process.

(1)

$$\mathtt{my\_fsum3} = -7{,}00 + 3{,}513\ \mathtt{DS\_SL} - 91{,}05\ \mathtt{DS\_SBK} - 12{,}90\ \mathtt{DS\_SBM}$$

(2)

$$\mathtt{ampl} = 0{,}004881 - 0{,}000831\ \mathtt{DS\_SL} + 0{,}005529\ \mathtt{DS\_SBK} + 0{,}004696\ \mathtt{DS\_SBM}$$

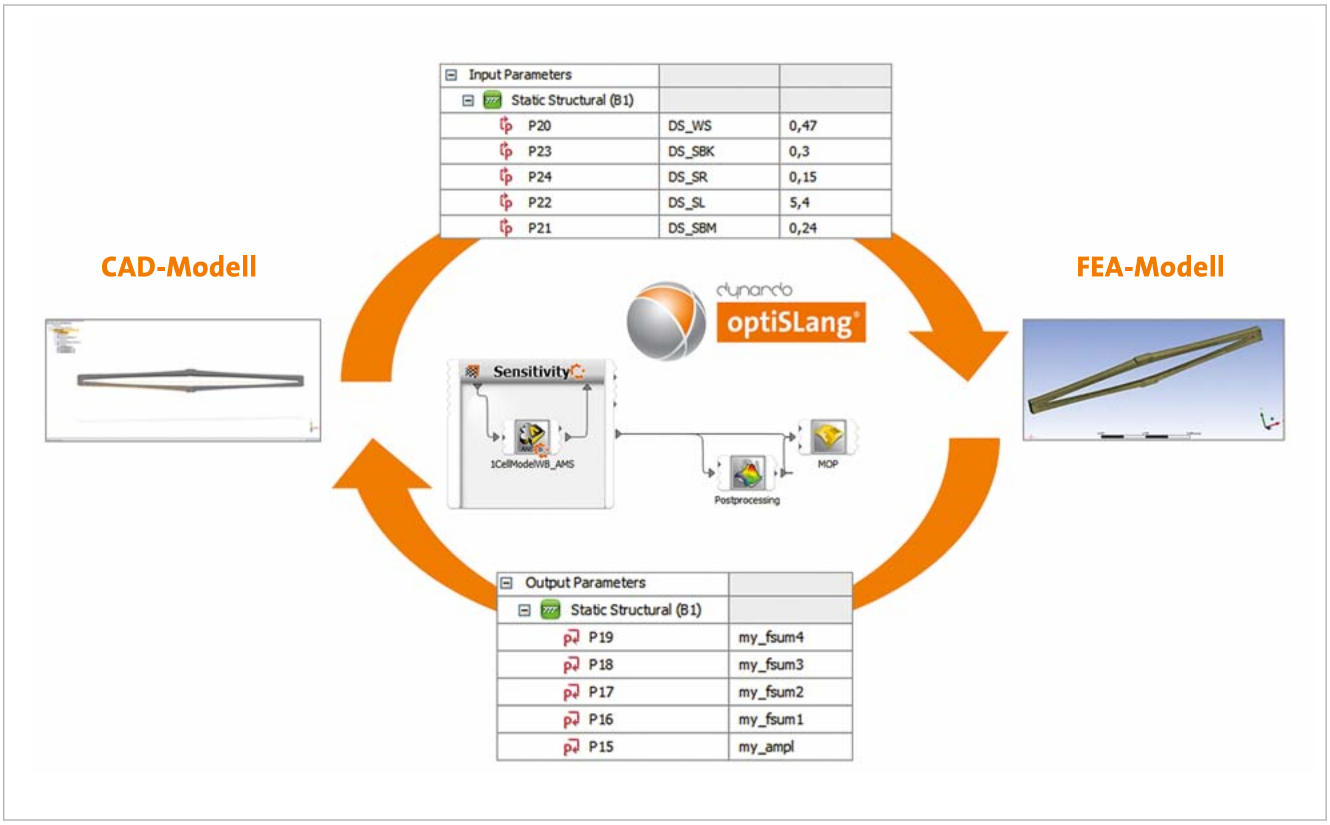

Fig. 2: Workflow including the different software tools

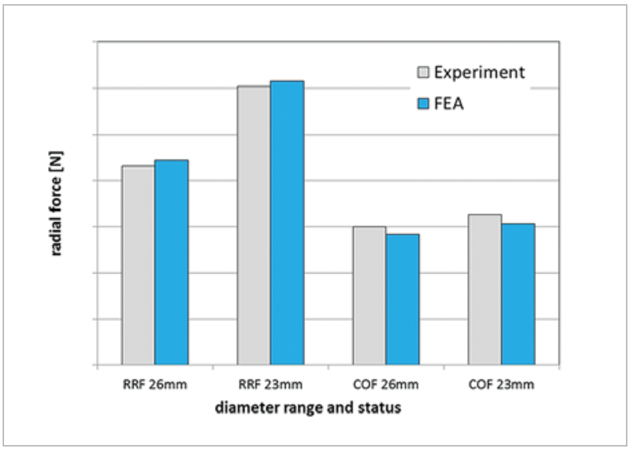

Fig. 3a: Comparison of experimental vs numerical radial force results for an exemplified stent design in a 23mm and 26mm vessel model

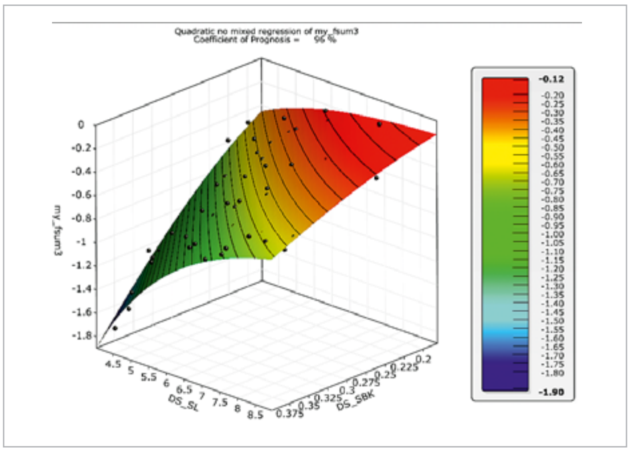

Fig. 4a: Radial force as function of strut length (SL) and strut thickness (SBK)

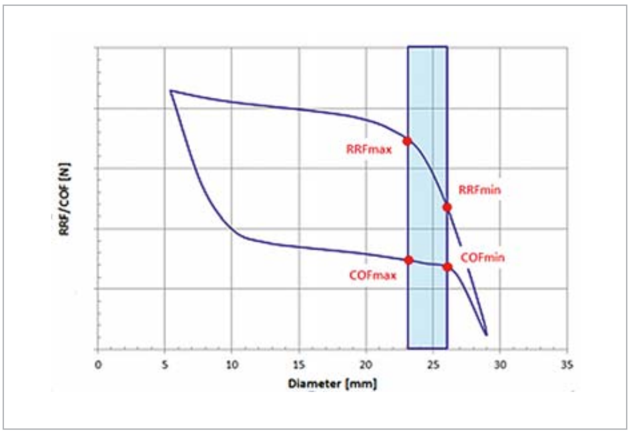

Fig. 3b: Evaluation points of the Nitinol curve

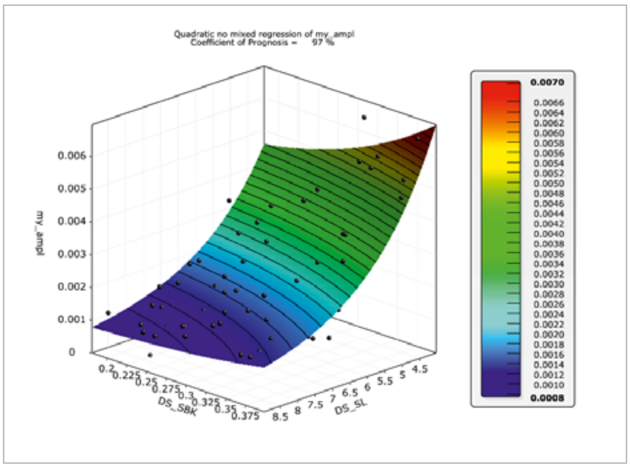

Fig. 4b: Strain amplitude as function of strut length (SL) and strut thickness (SBK)

	Experiment vs. FEA Delta [%]	Experiment vs. Statistics Delta [%]
RRF 26 mm	- 2.88	10.80
RRF 23 mm	- 1.92	5.84
COF 26 mm	5.73	- 11.66
COF 23 mm	6.36	- 9.90
Mean (absolute)	4.22	9.55

Fig. 3c: Comparison of experimental vs numerical (FEA) and experimental vs statistical (analytical) model

To improve the prediction of the linear regression model, the Metamodel of Optimal Prognosis (MOP) could be used which also allows the prediction of nonlinear response surfaces. The strut length has the largest influence on the radial force and strain amplitude and thus is one of the design driving variables (Fig. 4). The strut width near the radius is influencing the radial force while the strut width in middle has no clear effect on radial force but might be used to tune the crush resistance (torsional stiffness) of the stent.

The Design of Experiments and statistical modeling have the potential to support the initial design phase of cardiovascular devices in order to reduce time and costs for extensive FEA studies which are performed instead.

Authors//

Stephan Rothstock, Andre Hein, Karsten Koop
(Cortronik GmbH/Vascular Intervention)

Source//

www.dynardo.de/en/library

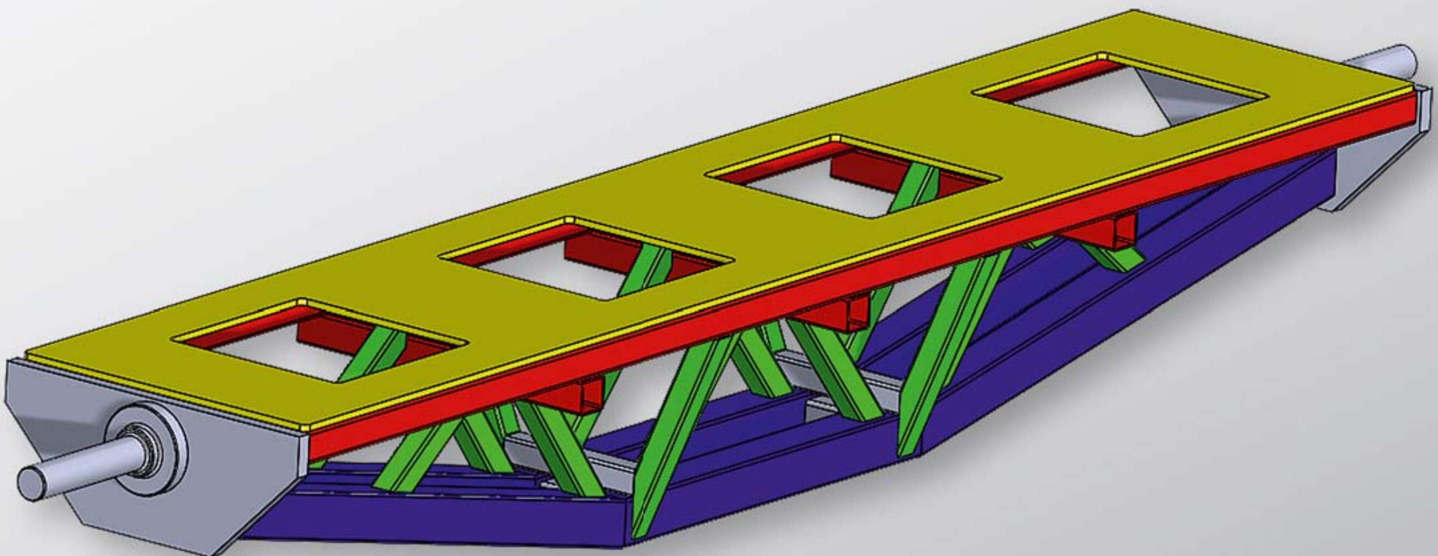

CASE STUDY // MECHANICAL ENGINEERING

MULTI-OBJECTIVE OPTIMIZATION OF THE WORK HOLDING DEVICE OF A MACHINE TOOL

The optimization of a work holding device regarding mass and deformation behavior was achieved with the help of a multi-objective optimization using optiSLang.

Task Description

The cover picture above shows the parametric CAD model of a work holding device with investigated geometric parameters of the upper (red), middle (green) and lower (blue) cross sections. The structure was represented by a parametric CAD model within ANSYS Workbench. The measure and thicknesses of the beams as well as the thickness of the upper plate were considered as geometrical parameters. Based on the CAD model, a finite element model was created by automatic meshing. Four lumped masses represented the work pieces while one external force was acting on one of the pieces to model the processing. Both shafts were modeled as fixed support. Three load cases were considered with the maximum deformation of the beam structure under 0°, 90° and 180° positions being calculated by the finite element model.

Minimizing the mass of the structure and the maximum deformation in all three load cases were the optimization tasks to be reached. The initial design had a mass of 207 kg and maximum deformations between 0,07 and 0,12 mm by using an aluminum plate and steel beams. With the help of a multi-objective optimization, first a suitable compromise between the optimization goals should be achieved. For this purpose, not only the beam cross sections should be modified but also different materials of the beam construction, namely aluminum ans steel, were investigated. Finally, the investigation should consider available standard beam measures out of a supplier catalogue in order to enable a cheaper production.

Design of Experiments (DoE) and Sensitivity Analysis

In a first step, the influence of the design parameters with respect to the mass and the deformations were analyzed. For this purpose eleven geometry parameters such as height, width and thickness of the upper, middle and lower beam cross sections as well as the thickness of the upper plate were varied within the defined boundaries. 200 parameter combinations were generated by the Advanced Latin Hypercube Sampling and evaluated by the finite element model for both types. From the 200 samples, only 10% failed as shown in Fig. 1 (see next page). The figure also illustrates that the failed designs occur if the height of the lower and upper cross section is too small. In such a situation, the external load could not be carried by the structure and the simulation model did not converge.

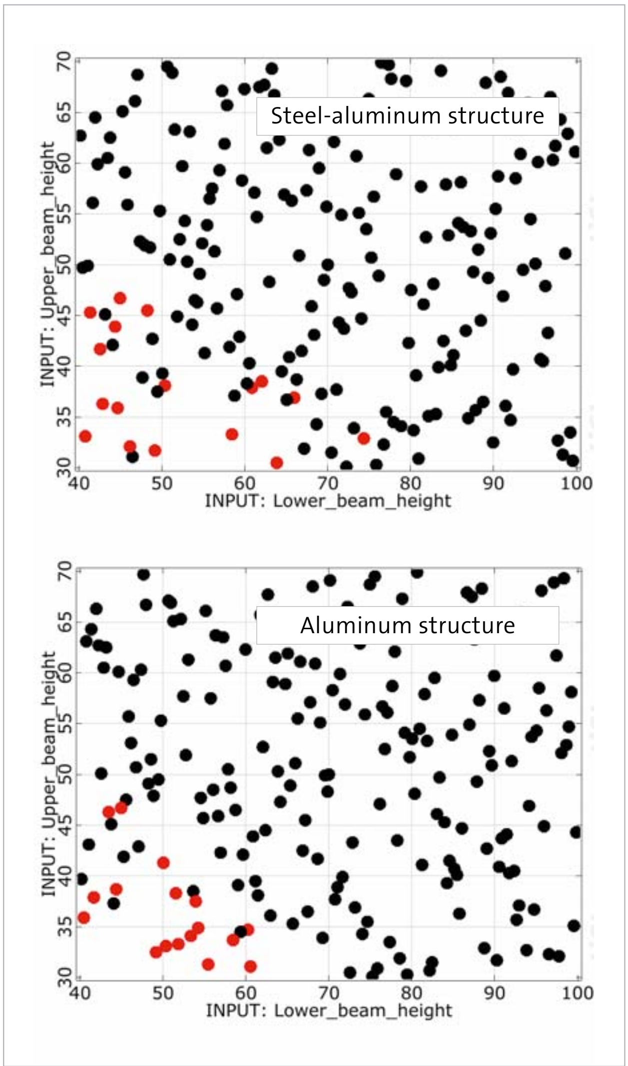

Fig. 1: 200 Latin Hypercube samples of sensitivity analysis with 10 % failed designs

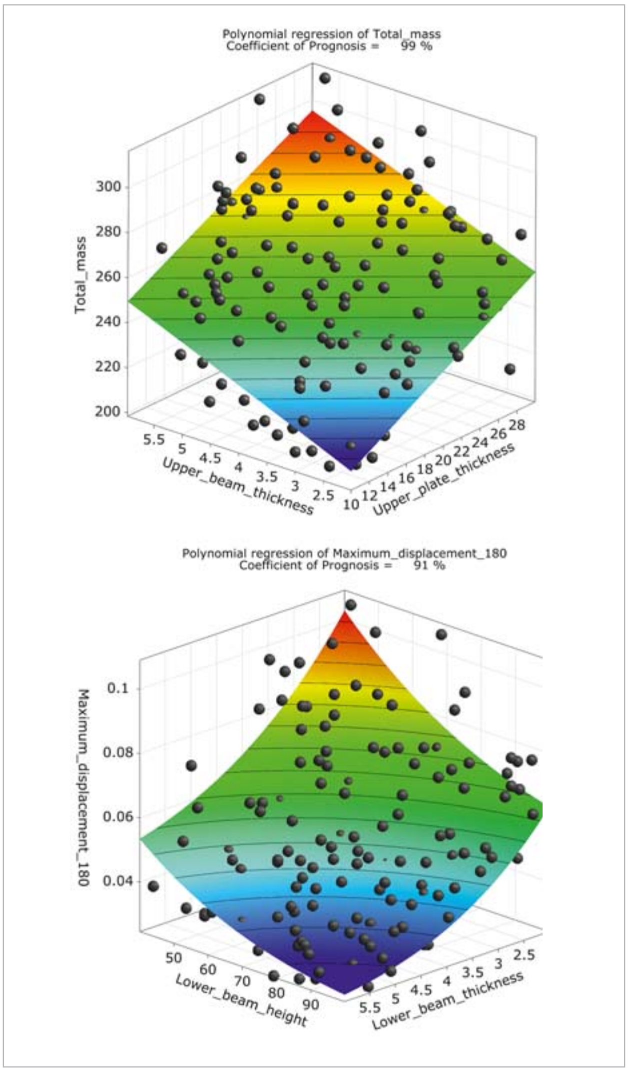

Fig. 2: Metamodels of Optimal Prognosis for the mass (top) and for the maximum deformation in 180°-position (bottom) for the steel-aluminum-structure

Thus, valid simulation results could be obtained in 90% of the design space. Using the Metamodel of Optimal Prognosis [Most 2011], the dependency of the mass and the deformations with respect to the variation of the eleven geometry parameters were quantified. The resulting optimal approximation models in the optimal subspace for the mass and one deformation value are exemplarily shown in Fig. 2. Meanwhile, the mass can be perfectly approximated with a linear polynomial model. The approximation quality quantified by the Coefficient of Prognosis with respect to the deformations is between 91% and 97%. The influence of the design parameters can be quantified sufficiently for each individual response value with the help of the MOP. In Fig. 3, the variance-based sensitivity indices with respect to the CoP are illustrated. The mass of both structure types is here mainly influenced by the thickness of the upper plate. However, the variation of the deformations can be mainly explained by the parameters of the lower beam cross sections. The influence of the distance between the lower beams is negligible, thus this parameter was kept constant in the following optimization.

Multi-Objective Optimization

In the next step, a good compromise between the different objectives was searched. For this purpose, the MOP was used as a solver surrogate within a multi-objective optimization. By using the evolutionary algorithm, the Pareto frontiers shown in Fig. 4 were obtained. The figure indicates that there is a clear conflict between mass and deformation but no conflict between the individual deformations. Furthermore, the figure clarifies that deformations less than 0.15 mm are not possible with the aluminum structure. Therefore, the steel-aluminum structure was preferred in the following analysis. Based on the identified Pareto-frontier, a maximum displacement of 0.1 mm was defined for all load cases.

Single-Objective Optimization

Using the results of the multi-objective optimization, a single-objective optimization was performed. As an optimizer, the Adaptive Response Surface Method [optiSLang 2016] was applied by minimizing the mass while the deforma-

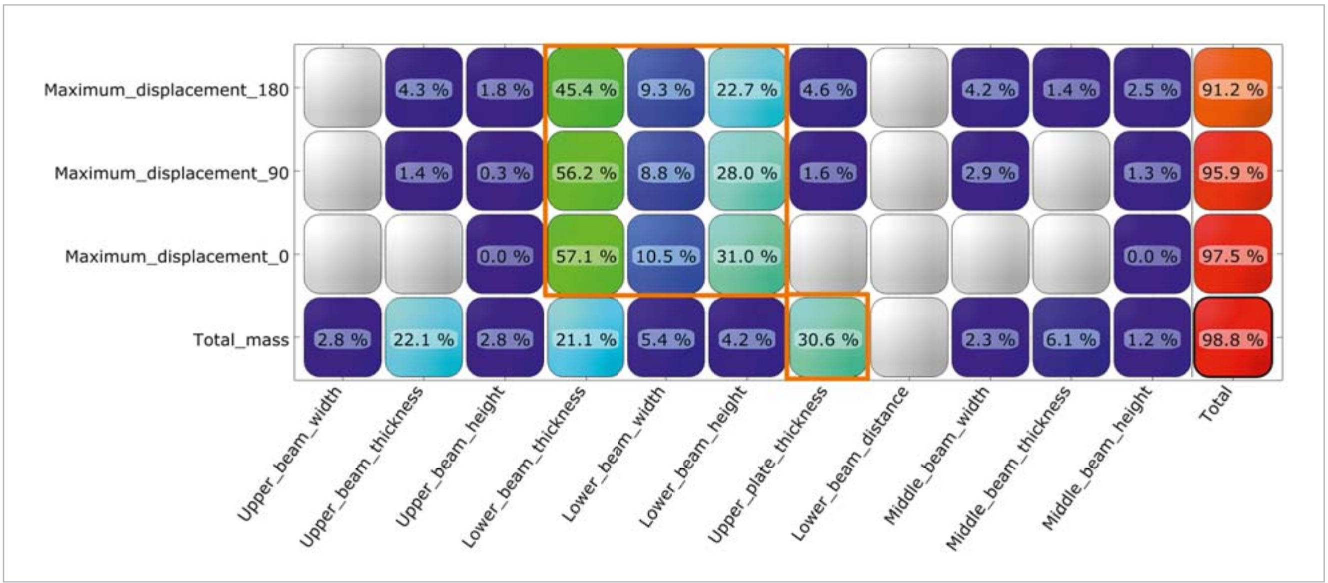

Fig. 3: MOP sensitivity indices of the design parameters with respect to the variation of the mass and deformations for the steel-aluminum-structure

tions of the three load cases were restricted to 0.1 mm. The convergence of the optimizer as well as the optimal design is shown in Fig. 5 (see next page). Compared to the initial design, a mass reduction of 10% and a reduction of the deformations in all three load cases of 17% were reached.

However, the best parameter combination is probably too expensive for production, because the optimal designs are based on arbitrary values and might not be available from standard suppliers. Therefore, the design parameters were defined as discrete parameters to enable the usage of standard cross sections. According to catalogue values [Thyssen 2015], the upper and middle beam cross sections were defined as quadratic with possible values for width and height of 30, 40, 50, 60 and 70 mm. The available thickness values of these beam elements ranged between 2, 2.5, 3, 4 and 5 mm. For the lower profiles, cross section values of different width and height with 40, 50, 60, 80 or 100 mm were selected with thickness values of 2.5, 3, 4 or 5 mm. The optimization again was performed with the Adaptive Response Surface Method. The results are shown in Fig. 6 (see next page). Due to the lower flexibility in the optimization task, the mass was reduced only by 7%. Nevertheless, due to the usage of cheap standard beam cross sections, the production cost is much less compared to the optimal design of the previous optimization.

Summary

Based on a parametric geometry model the deformations of the work holding device were calculated by a finite element model. Since, a priori, weighting of the different objective function was not possible, a multi-objective optimization was performed first. Based on these results, a single objective optimization problem could be formulated by defining a maximum deformation constraint. Compared

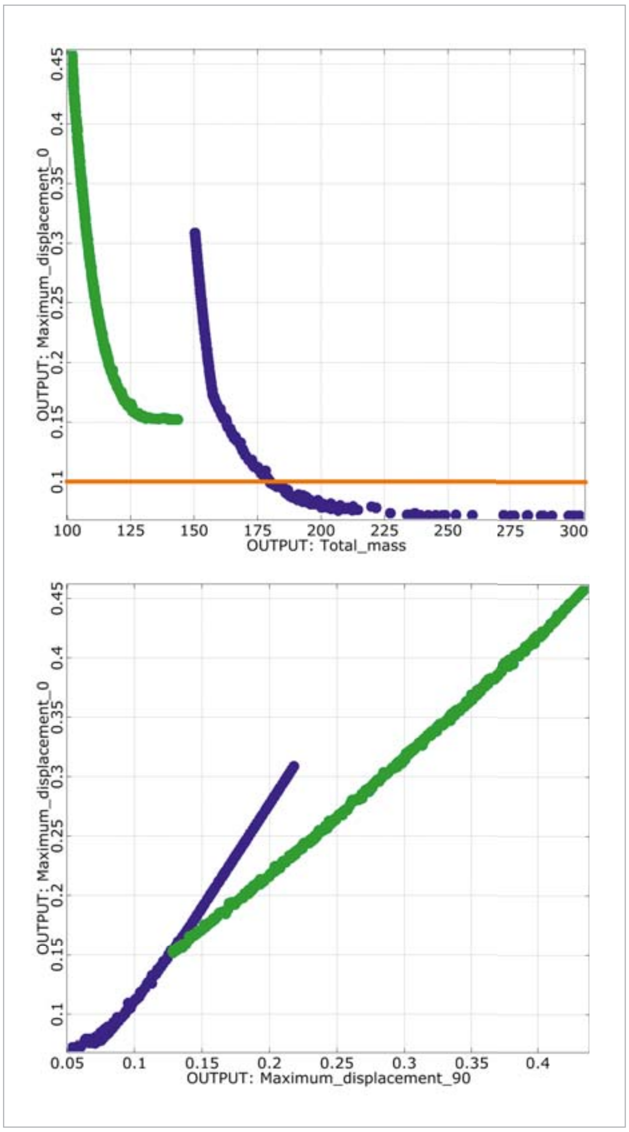

Fig. 4: Pareto-frontier of the multi-objective optimization: mass and deformation show a clear conflict (top), the individual deformations show no conflict (bottom) | green=aluminum / blue=steel

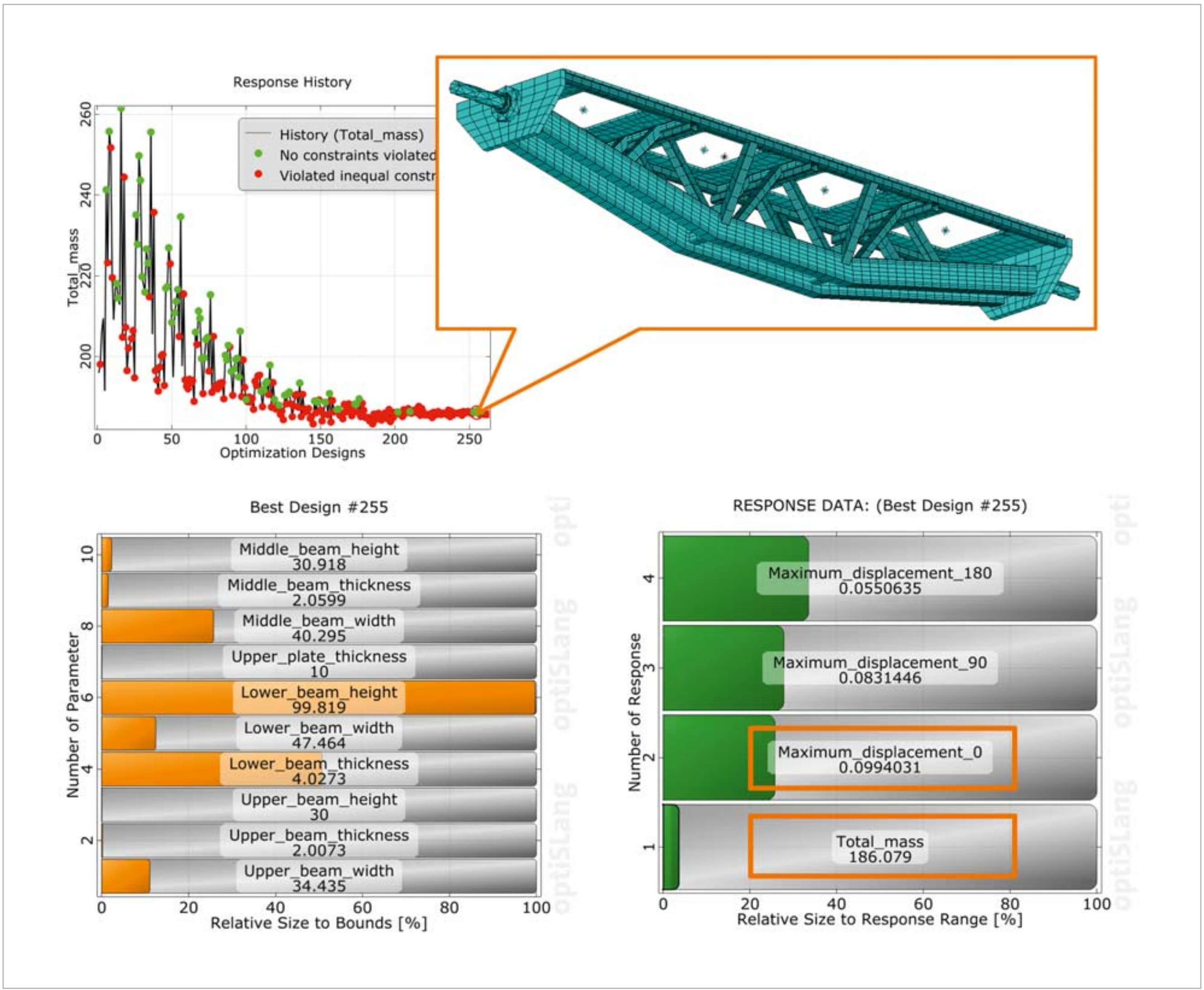

Fig. 5: Single-objective optimization with continuous design parameters – optimizer convergence and best design

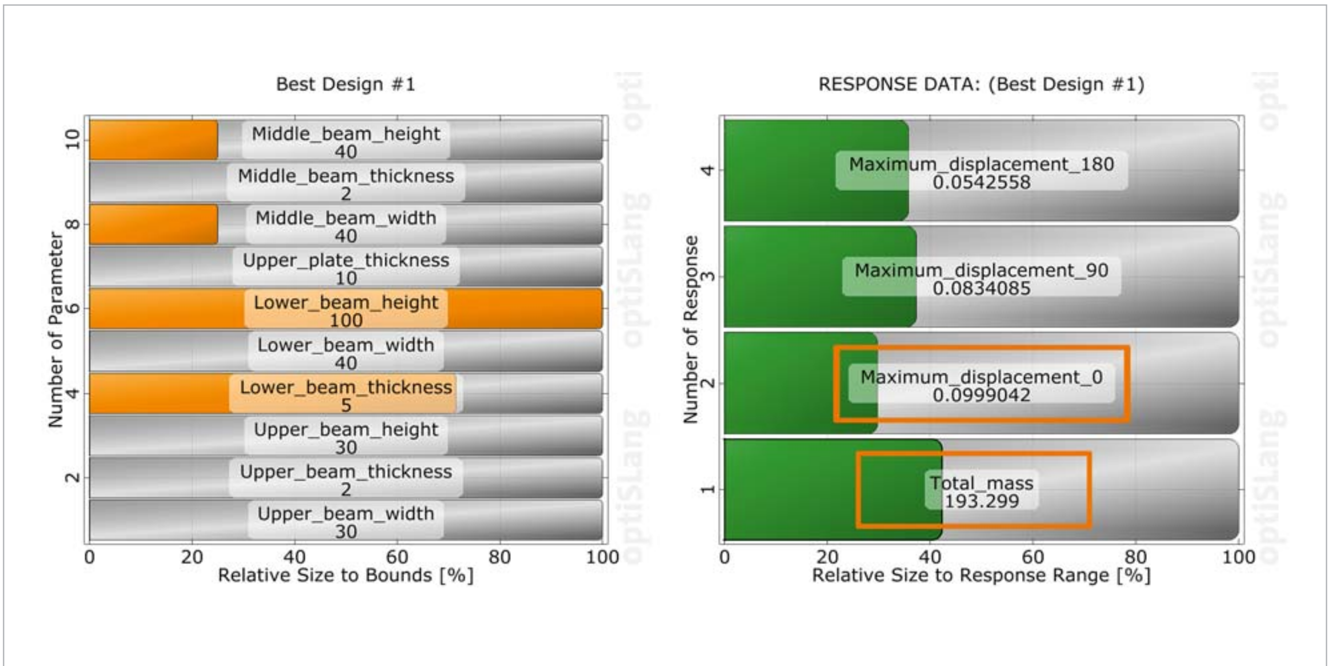

Fig. 6: Best design of the single-objective optimization using discrete design parameters

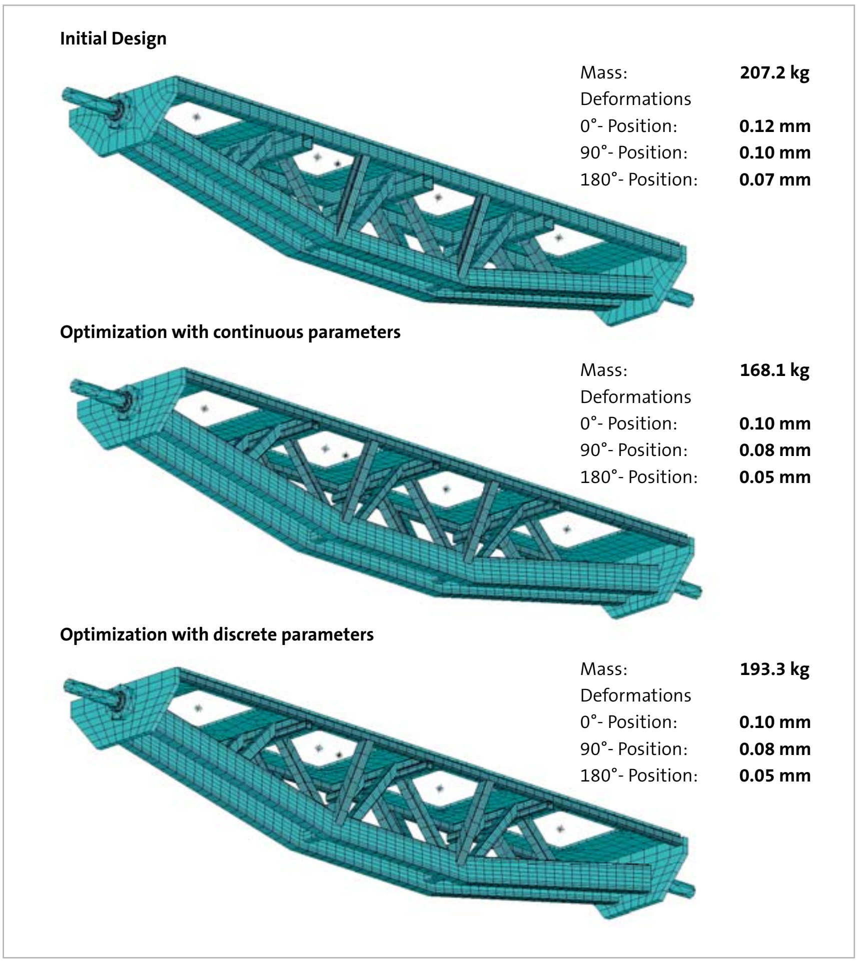

Fig. 7: Summary of the results of the two optimization steps

to the initial situation, the mass could be reduced by 10% and the maximum deformations by 17%. In order to allow a cheap production, the design parameters were finally formulated as discrete parameters considering the standard beam measures of a supplier catalogue. With this setup, the mass could be reduced by 7% and the deformation by 17%.

Authors //
Thomas Most (Dynardo GmbH) /
Jochen Burkhardt,
Christoph Birenbaum
(Fraunhofer Institut für Produktionstechnik und Automatisierung
Stuttgart)

References //

[Most 2011] Most, T. & Will, J., "Sensitivity analysis using the Metamodel of Optimal Prognosis", Proceedings Weimar Optimization and Stochastic Days 8.0, 2011

[optiSLang 2016] Dynardo GmbH, „Methods for multi-disciplinary optimization and robustness analysis", optiSLang documentation, Version 5.1, 2016

[Thyssen 2015] ThyssenKrupp Schulte "Kaltgefertigte Stahlbau-Hohlprofile", Product catalogue, www.thyssenkrupp-schulte.de, 2015

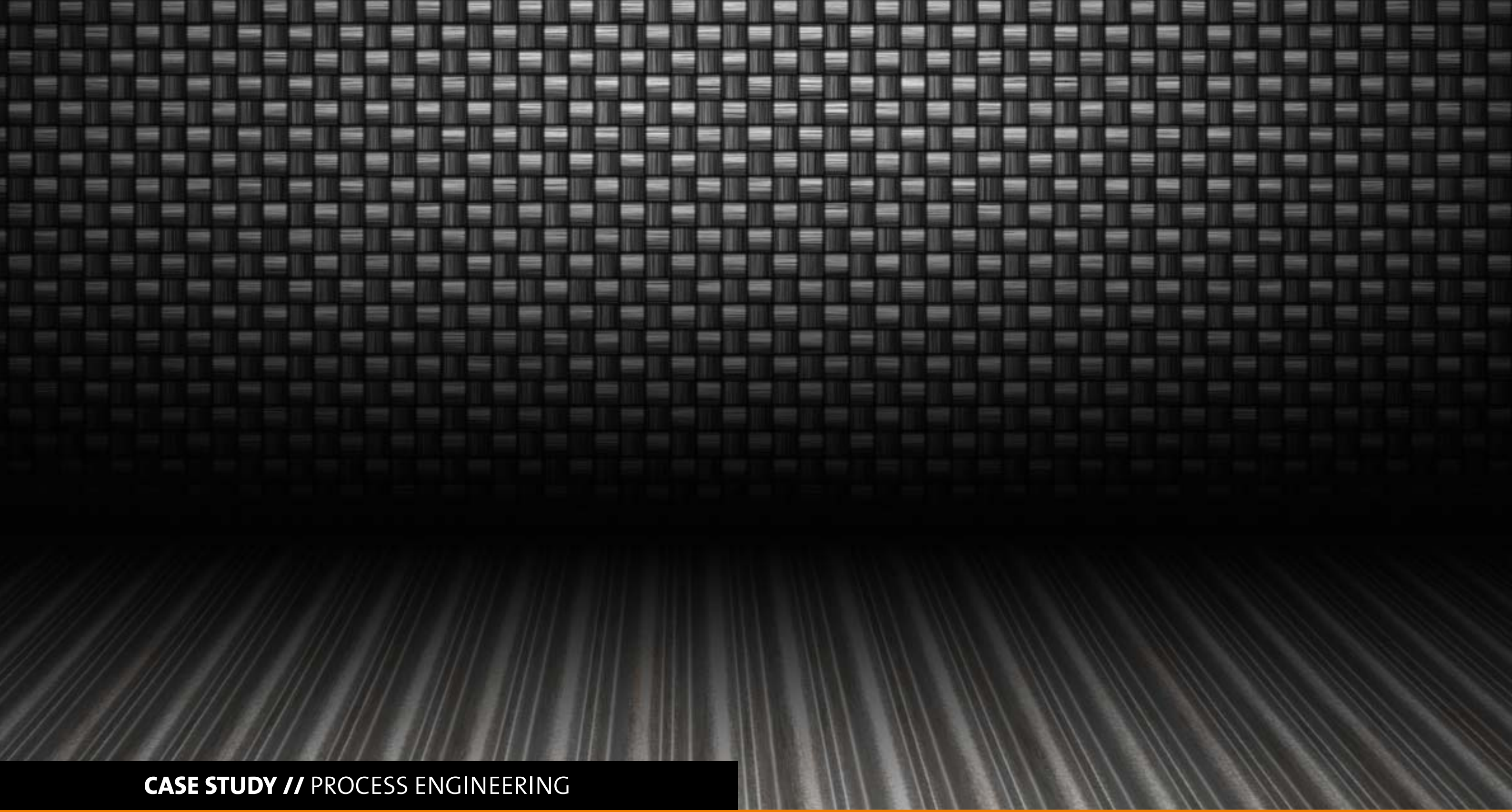

SIMPLIFIED SIMULATION OF ALUMINUM-CFRP ADHESIVE JOINTS

optiSLang supports CAE-based simulation of hybrid adhesive joints by appropriate methods of model reduction using correlation models.

A detailed simulation of the non-linear behavior of adhesive joints is often not possible in regard to model complexity and computation time. If it becomes necessary in product development to simulate this non-linear behavior, reduced correlation models must be generated. As part of a funded research project, Brose Fahrzeugteile GmbH & Co. KG, CADFEM GmbH, Dynardo GmbH and the Chair of Engineering Design of the Erlangen-Nuremberg University investigated such correlation models (hereinafter referred to as meta-models) and their calibration regarding the capability of generating a sufficient prognosis of the nonlinear structural behavior of adhesive joints within reasonable computational effort and accuracy. After a successful calibration of appropriate meta-models, the economic use of numerical simulation and computer aided design methods for adhesive joints already becomes possible in an early stage of product development.

Compounds of aluminum and Carbon Fiber Reinforced Plastics (CFRP) achieve tremendous advantages for lightweight applications through the optimal utilization of the material properties. For example, this compound can be found in lightweight door modules (see Fig. 1) where aluminum parts like window lifter rails are applied to a door module made of CFRP.

Fig. 1: Light weight door module | © Brose Fahrzeugteile GmbH & Co. KG

The properties of such hybrid structures decisively depend on the joints between the component parts. This makes a sufficient load and material related design of these joints very essential. However, the anisotropic material behavior and a tendency towards delamination of the CFRP, as well as differing coefficients of thermal expansion of the joining structures make this aim hard to achieve. The fulfillment of requirements such as sufficient robustness towards varying thermal conditions or crash safety regarding the joints is only reachable if CAE-based procedures are implemented at an early stage of product development.

The basic steps of the derivation and calibration of correlation models of adhesive joints are shown in Fig. 2. Within the loading conditions of the joints, a design of experiment and a test setting is defined. At the same time, a parametric simulation model is created for the recalculation of all tests. The unknown or uncertain material parameters of the simulation model are calibrated on the test results. Thus, if an adequate prognosis capability is achieved, a large number of experimental set-ups can be virtually calculated to generate a sufficient data base for a predictive correlation model.

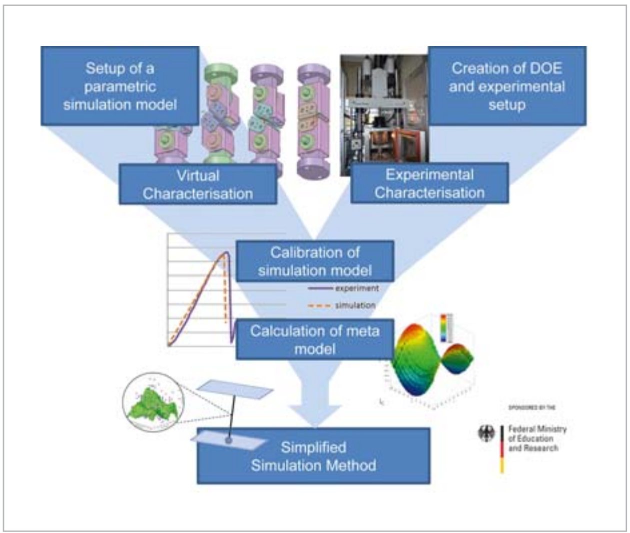

Fig. 2: Approach for the generation of a simplified simulation method

The reduced model is then used for modeling the adhesive joints on the contact elements. Thus, while having access to the data base of the meta-model, the modeling effort for a detailed simulation can be saved. The steps of generating a simplified simulation model, in particular the experimental and virtual characterization of the adhesive joints as well as the final validation of the simulation method, will be discussed more detailed in this article.

Experimental setup

To characterize the adhesive joints, a modified KS2-sample is used (see Fig. 3). In this case, a polyurethane adhesive joint of an aluminum and a CFRP plate is tested under the condition of production temperature, processing and hardening. The tearing experiment is carried out at a servo-hydraulically operated test facility (see Fig. 3). To carry out the high and low temperature tests, there is a temperature chamber integrated in the test facility. The force-displacement curves are recorded as the basis for later calibration with the simulation.

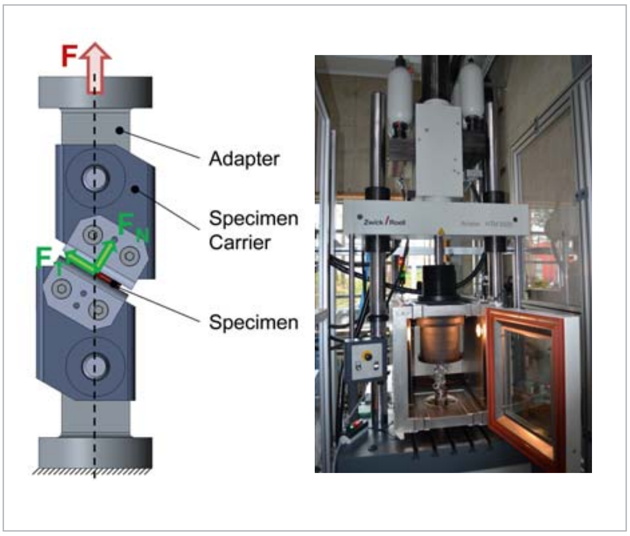

Fig. 3: Test design and facility

Parameter space to describe the possible operating conditions

Usually, the number of real experiments to be carried out should be minimized and, consequently, a minimalistic DOE has to be created. Here a linear D-optimal experimental design is chosen. Table 1 shows the parametrization and Fig. 4 (see next page) illustrates the sampling points in a 3-dimensional subspace.

Parameter		Values			
Joint Width (mm)	x_1/d	0,3	0,6	1	
Layer structure	x_3/LA	1	2		
Load angle (°)	x_4/α	0	45	60	90
haul-off speed (m/s)	x_5/v_α	0,001	0,1	2	
Temperature (°C)	x_6/T	-30	23 room temp.	80	

Table 1: Values of parametrization

As relevant parameters for simulating various load scenarios, the setting angle in regard to the direction of tension, the test speed and temperature, the thickness of the adhesive seam as well as different layer structures of the CFRP laminate are varied in the testing. Using the result variables of the thirty testing procedures of the experimental design, the most dominating major effects such as the acceptable force and displacement as well as the test speed and temperature can be identified.

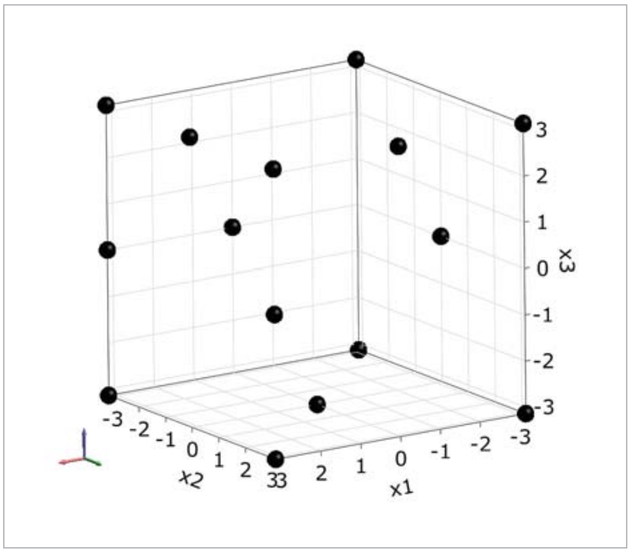

Fig. 4: Sampling points in a 3-dimensional subspace

Fig. 5 shows the Coefficient of Prognosis (CoP) and the Metamodel of Optimal Prognosis (MOP) for the maximum acceptable load and Fig. 6 represents the corresponding displacement derived from the thirty experimental procedures.

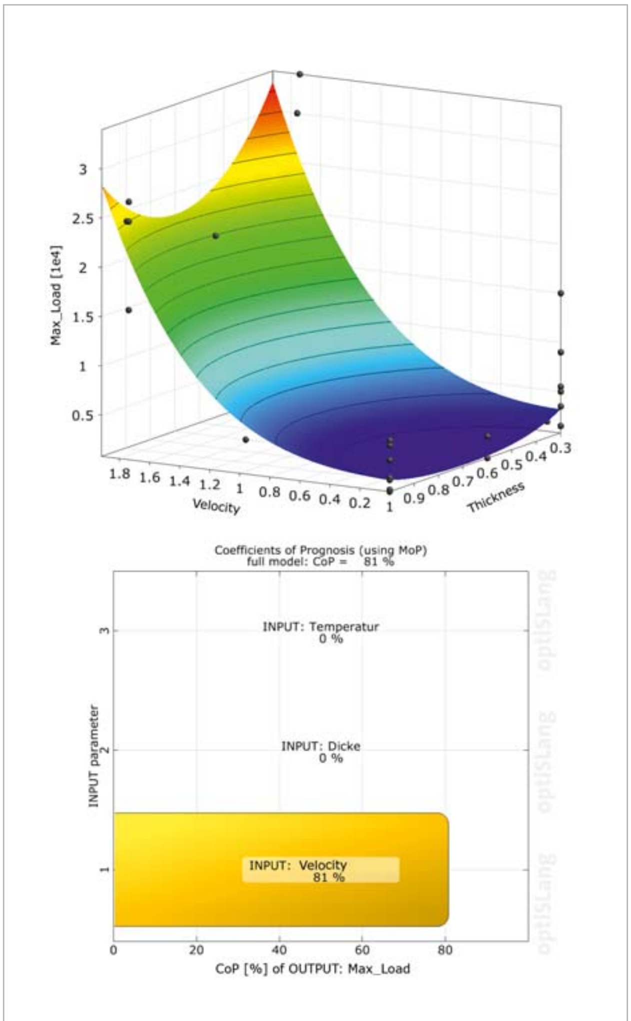

Fig. 5: MOP and CoP of maximum acceptable load

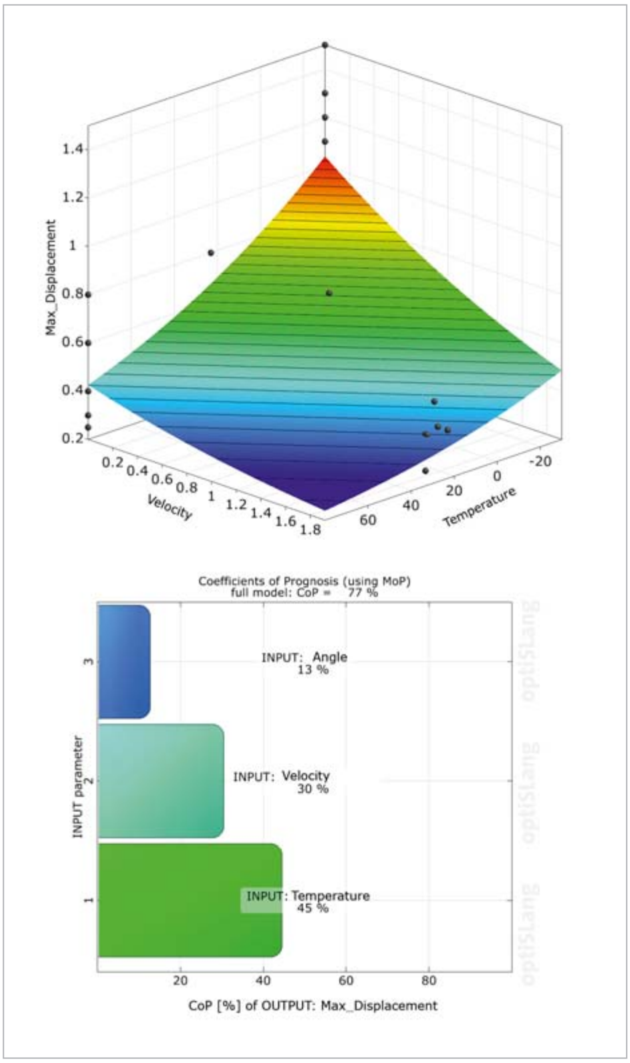

Fig. 6: MOP and CoP of the corresponding displacement

Detailed simulation

The results of the experiments serve as calibration points for the detailed simulation. Here, the failure modes that occur in practice have to be covered. Fig. 7 represents the failure of the adhesive joint on the aluminum surface, the cohesive failure within the adhesive layer and the delamination of the CFRP layer structure. The simulation model is designed as a parametric geometry model enabling the angle of the clamped specimen, along with the thickness of the adhesive layer to be varied. The possible variations of the angle ranges from 0 ° to 90 ° in regard to the tensile axis and the adhesive layer thicknesses can be varied from 0.3 to 1.0 mm. Regarding the adhesive layer, a viscoelastic material behavior is selected that also shows a different behavior when changing the temperature. For simulating the adhesive failure on the aluminum surface as well as the delamination in the CFRP layer structure, contact elements with cohesive zone approaches are used in the simulation model. The individual CFRP laminate layers, according to their thickness and fiber orientation, are each meshed with one layer of three-dimensional elements, as shown in Fig. 8. Adhesive and aluminum are also modeled with three-dimensional elements over the thickness and marked with the cor-

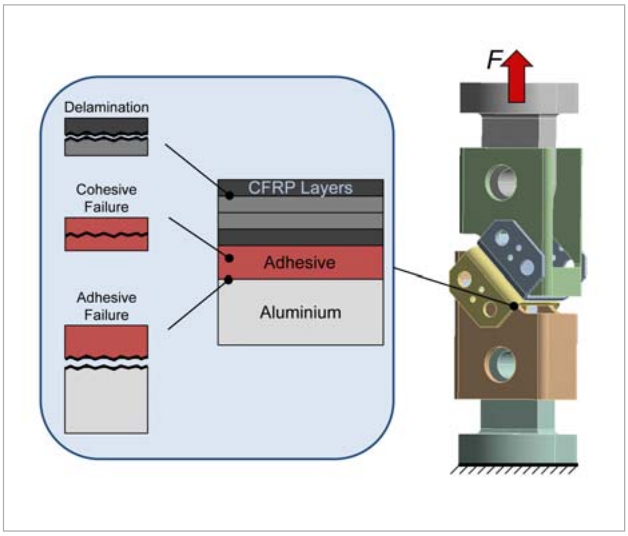

Fig. 7: Modes of failure of the adhesive joint

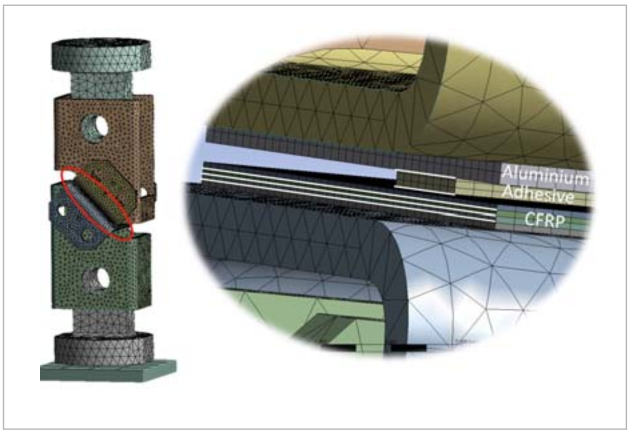

Fig. 8: Meshing of the adhesive joint

responding material properties. After an initializing step, the model is then driven with the defined speed until one of the described failures occur. The material parameters of the separating layers, the failure criteria and the damping parameters are based on assumptions in the first instance. They have to be determined by means of parameter identification.

Model calibration

Important parameters to be calibrated comprise the maximum contact normal stress, the critical fracture energy density in normal direction (surface energy), the maximum equivalent tangential contact as well as the critical fracture energy density. A total of 25 parameters have to be identified in order to achieve an adequate correlation with the thirty test models. The unknown material parameters have to be calibrated in regard to the experimental results with the help of the numerical simulation model and an inverse approach. The identified material properties and the calibrated simulation model are then used to calculate a sufficient number of support points for the mathematical surrogate models.

Unfortunately, standard procedures such as the minimization of error squares, could not be successfully applied during the calibration. Due to the many unknown variables and the partially highly sensitive behavior of the simulation model, the parameter ranges were limited gradually. A fully automatic optimization method could not be applied for each adaptation step. Therefore, quasi-random experimental designs were used to scan the subspace and to identify appropriate parameter combinations. With the help of the Latin Hypercube Sampling and the parallel coordinate plot,

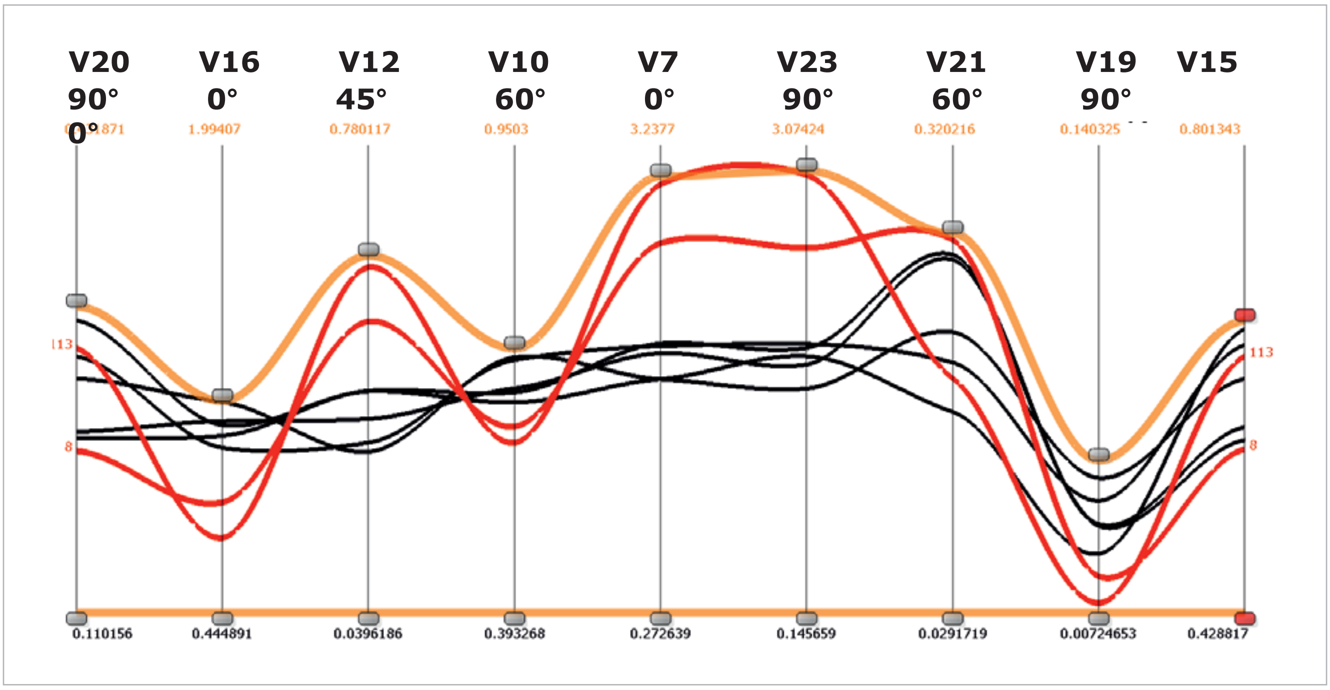

Fig. 9: Parallel coordinate plot

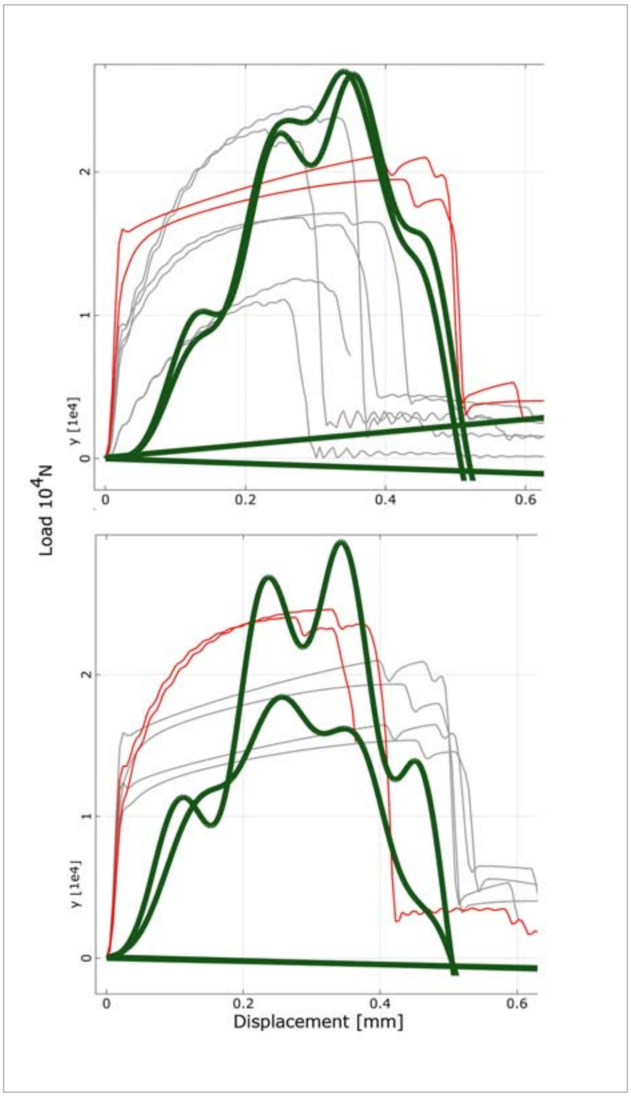

Fig. 10: Calibration of the detailed model to the experimental curves for a test with only tensile stress (top) and a test with mixed tensile and shear stress (bottom)

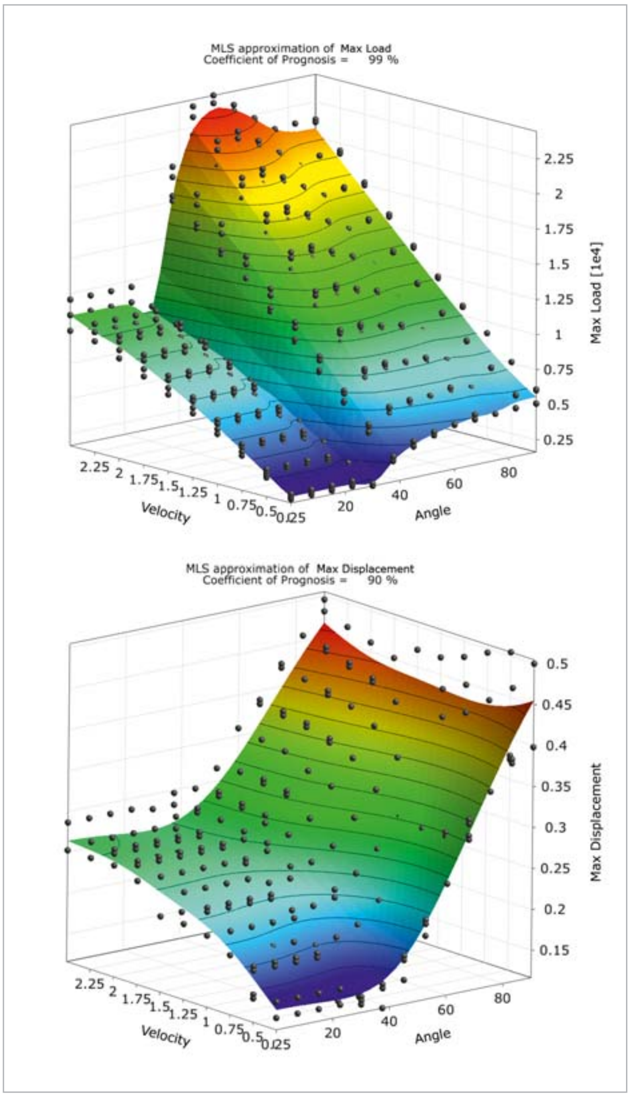

Fig. 12: Derived MOPs for max load and corresponding displacement

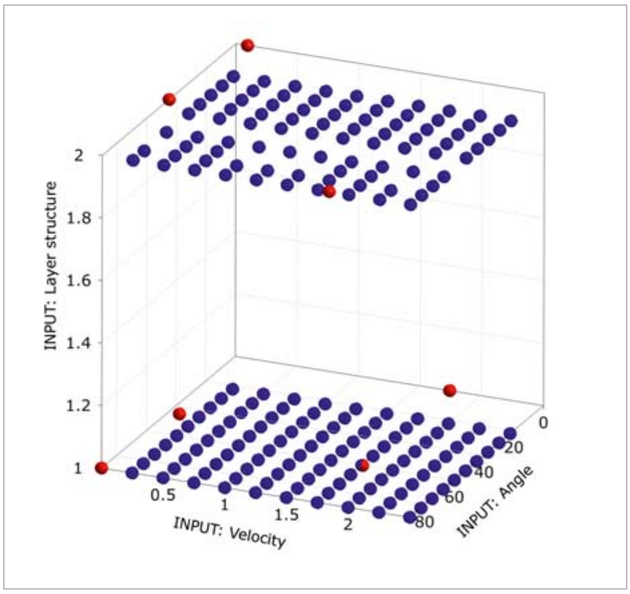

Fig. 11: Comparison between experimental parameters and the successfully calculated results of the simulation

an incredibly efficient evaluation of the quality of each parameter combination according to various criteria was possible. Fig. 9 (see previous page) shows the limited range of the simulation results with a sufficient calibration.

Thus, a sufficient calibration between experiment and simulation was achieved and the associated surrogate models could be derived. Fig.10 shows the experimental data compared to the simulation results for the experiments at high loading velocity.

Generation of the meta-models

The matching in regard to displacement and maximum load between the experiments using the calibrated simulation models was 88 percent higher than the results of the experimental data with 77 and 81 percent, (see Fig. 5 and 6). After the verification of the calibrated parameter set was determined as being capable of a sufficient approximation of the test results, an adequate number of sampling points

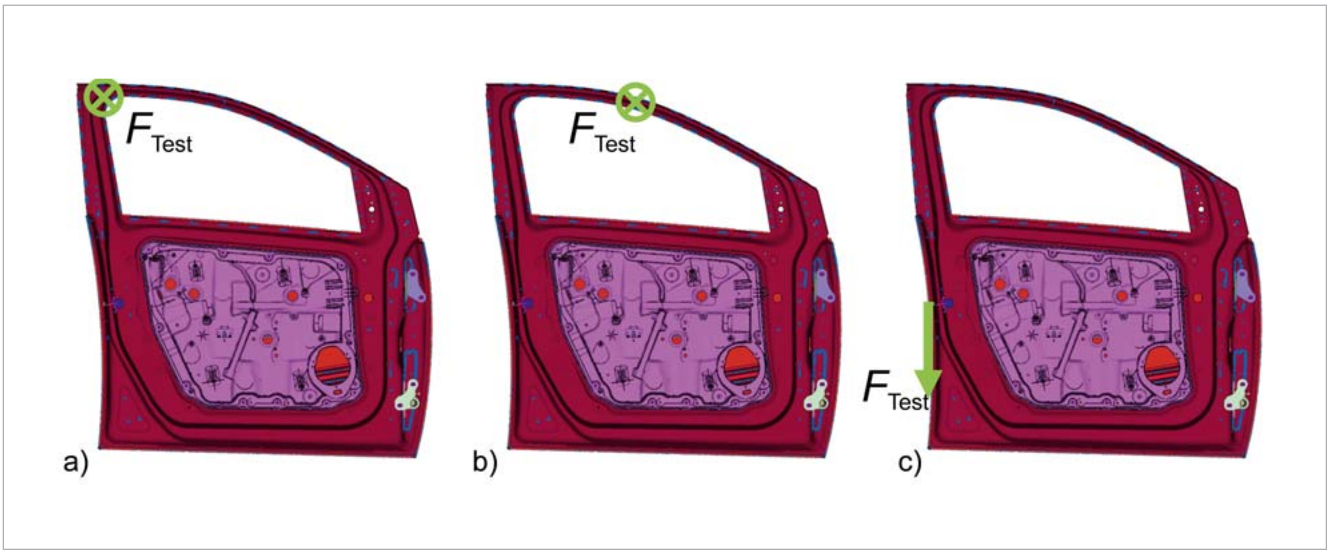

Fig. 13: Load cases for validation; frame rigidity (a and b); door lowering (c) | © Brose Fahrzeugteile GmbH & Co. KG

were calculated using additional virtual experiments. According to the application case, the temperature at 23 ° C and the adhesive thickness with 0.3 mm were considered constant. The remaining parameters regarding layer structure, speed and angle were entirely scanned by using a full factorial DOE scheme. Fig. 11 shows the comparison between experimental parameters and the successfully calculated results of the simulation.

The calculated result values for each parameter combination enable the generation of meta-models for the maximum load with a prognosis quality (CoP) of 99% as well as for the associated displacement of 90% (see Fig. 12). The meta-models are integrated within a finite element in an implicit and explicit simulation tool. The created meta-model continuously describes the correlation between the stress situations and the contact behavior and can be accessed within the FE simulation.

Validation

The validity of the simplified simulation approach is examined by comparing it with the component tests of vehicle doors. The points of load application are located on the upper frame near the B-pillar and on the middle frame (see Fig. 13 a and b). In both load cases, the system stiffness significantly depends on the design of the joint. To take account of highly dynamic load cases, tests are carried out which are designed to simulate an accident scenario. Such side impact tests on vehicle doors are conducted and evaluated according to typical automotive specifications.

Summary

With the simplified simulation of adhesive joints based on meta-models, it is possible to significantly reduce the amount of calculation for the evaluation of product characteristics in early stages of development. The presented method is considered to be general and can also be applied to other types of compounds along with other adhesives or joining methods, such as riveting.

It should be noted that the generation of a predictive meta-model requires a minimum number of experiments for every variation window combined with a large number of simulated design points using a suitable simulation model. Important for the prognosis quality of the meta-models is the quality of the design and the setup of the experiments as well as the quality of the numerical model covering the main physical phenomena. The calibration, the verification of a sufficient prognosis quality, the design of virtual experiments and the derivation of meta-models can be automated by using optiSLang and, thus, combined with today's High Performance Computing capabilities, can be considered as relatively minor efforts in cost and time.

Authors//

Prof. Sandro Wartzack, Christian Witzgall
(Friedrich-Alexander University of Erlangen-Nuremberg) /
Markus Kellermeyer (CADFEM GmbH) /
Thomas Most (Dynardo GmbH)

Thanks for the support of the executing project organization at DLR Berlin, thanks to the Federal Ministry of Education and Research for funding the research project Real4Hybrid (number 01 | S13009D) and also thanks to all project partners for their fruitful cooperation.

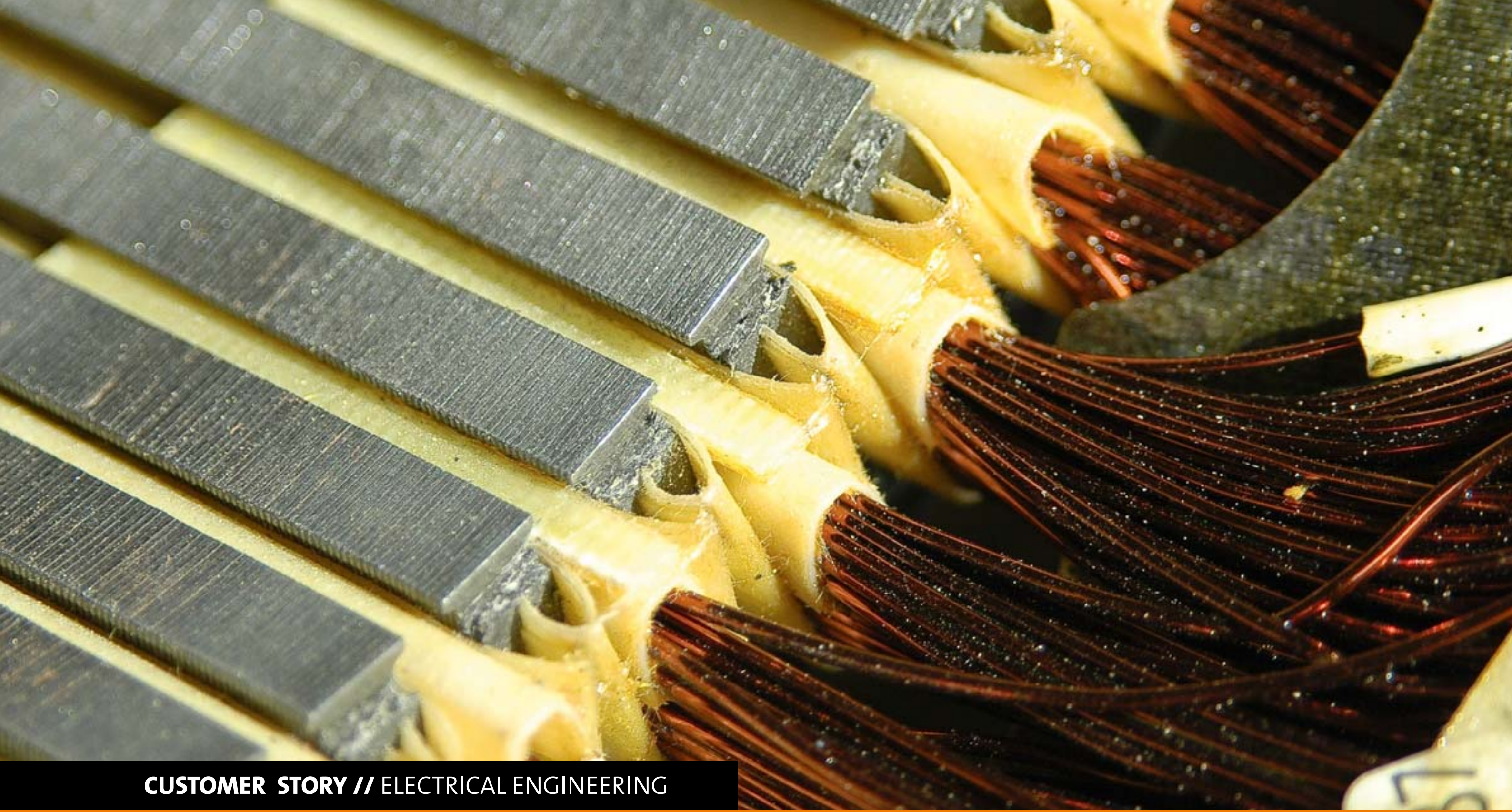

CUSTOMER STORY // ELECTRICAL ENGINEERING

SIMULATION OF COPPER WIRE WINDINGS IN ELECTRIC MOTORS

The application of optiSLang enables the verification and optimization of material models for an improved simulation of the material behavior of copper wire windings in electric motors.

Introduction

The simulation of heterogeneous materials makes high demands on the calculation regarding computing time. Approaches of idealization are often used to minimize computational time, but should also be capable of describing the behavior of the components precisely. The result of such idealizations is a synthetic material model. The general intention is to verify and optimize the model with the help of appropriate tests.

This article describes such a procedure using the example of windings for electric motors. These windings are made of copper wires embedded in a matrix material consisting of impregnating resin. The impregnating resin serves as a mechanical stabilizer, electrical insulation and heat dissipation. The copper wires conduct electricity and thereby generate the magnetic field for the motor. Modelling individual wires in the simulation would lead to an extremely large amount of computing time and model size. Thus, an idealization of the windings in the simulation model is normally unavoidable.

In literature, two different approaches can be found for idealization. One uses the approach of Chamis, which specifically applies for the simulation of plastics. Another option is the approach of continuum mechanics, which is mainly used for inhomogeneous materials such as concrete or short-fiber-reinforced plastics.

For the verification of the obtained material, a simple bar shaped specimen is extracted from the windings of the electric motor. The so-called slot bar is taken from the area between the teeth and the slots of the lamination stack.

Methodology

Idealization and FE simulation

For the idealization of the component behavior, the continuum mechanics approach of micro and macro structures is used. In this case, the macro level describes the global behavior of the body. For the micro level, a point of the macro level is defined which represents all points of the macro level, the so-called Representative Volume Element (RVE). The approximation of homogeneous material properties in the macro-level and a sufficiently small microstructure

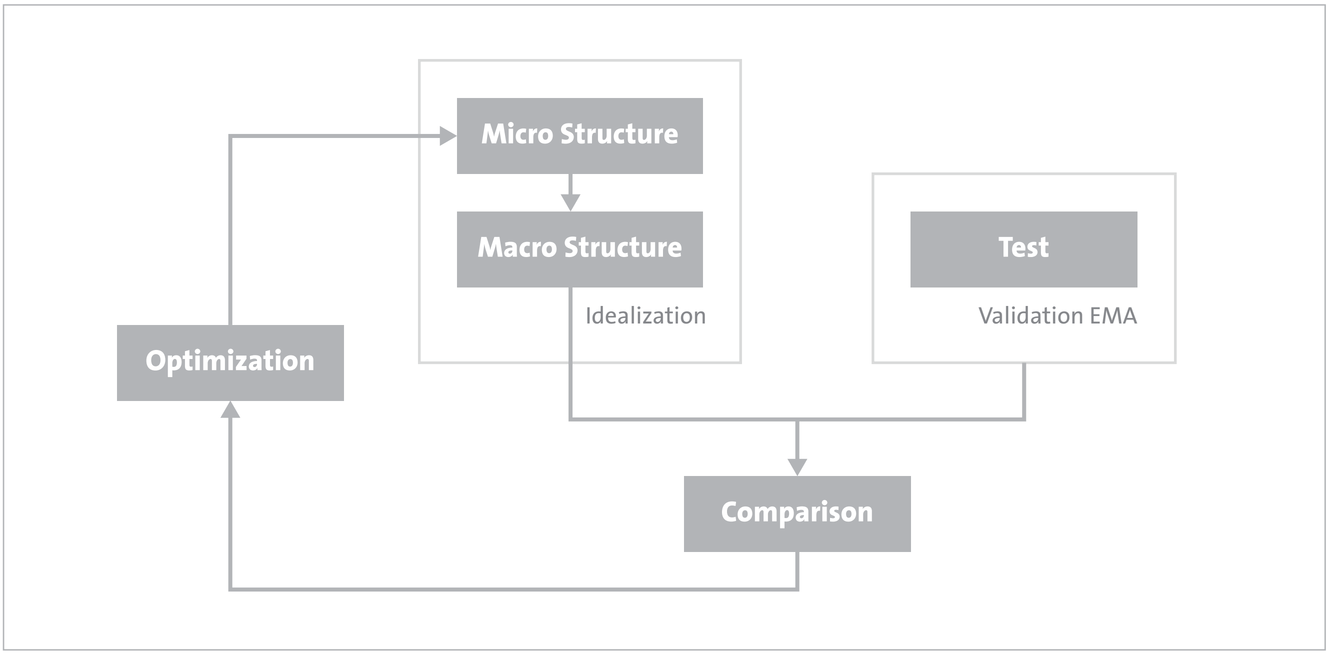

Fig. 1: Flow chart

enables the derivation of the RVE constraints. If the RVE is now exposed to deformation loads, its stiffness matrix can be determined. The so considered anisotropic material can be used for calculating the macroscopic structure.

Using this structure, an idealized material is defined having the same characteristics as the real component. Afterwards, for the slot bar, a computational modal analysis is carried out with this idealized material. The experimental modal analysis serves as a reference test.

The calculation and measurement are compared by using the MAC criterion and the material parameters are optimized regarding the test results. The flow chart of this process is shown in Fig.1.

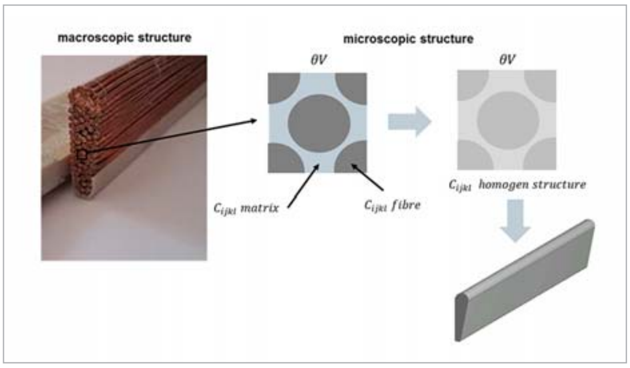

Fig. 2: Homogenization

The values of Young's modulus and Poisson's ratio are taken from literature and serve as initial values for the copper wire. Impregnating resins are specifically developed for the usage in electrical machinery, usually as epoxy resins. The material is properly adapted referring to the later application of the engine and its manufacturing. Epoxy resins have time and temperature independent properties and are viscoelastic. The determination of the initial values is performed by measurements on the resin samples also taking into account the independency regarding temperature and time.

With the help of these output values, the homogenization of the slot bar is conducted. The obtained anisotropic material model is used in the computational modal analysis of the slot bar.

Reference test

For the calibration of the calculated modes, the experimental modal analysis is used. The slot bar is set to oscillate freely by mechanical excitation. The amount of excitation and the resonant response are measured at various points on the bar. The transfer functions for the determination of modal sizes, natural frequency and eigenmode can be derived from the difference between the input and output signals. The measured eigenvalue is then compared to the calculated ones from the simulation.

In this case, the measured mode shapes intended to be used for verification are the first three bending vibration modes and the two torsion mode shapes shown in Figure 3 (see next page).

Calibration of eigenvalues

The Modal Assurance Criterion (MAC) is used for the comparison of the mode shapes with

$$MAC = \frac{[\emptyset_i \cdot \emptyset_j]^2}{[\emptyset_i \cdot \emptyset_i] \cdot [\emptyset_j \cdot \emptyset_j]}$$

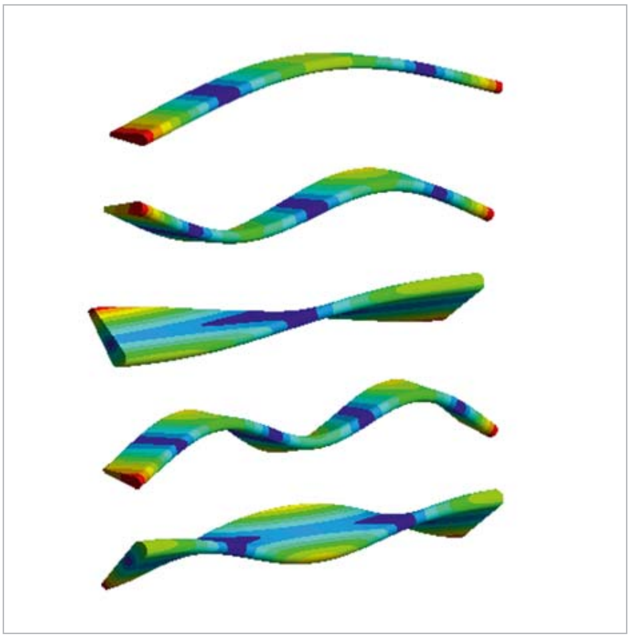

Fig. 3: Mode shapes of the slot bar | top down - 1st bending, 2nd bending, 1st torsion, 3rd bending, 2nd torsion

The comparison of the Experimental Modal Analysis (EMA) with the simulation of the bar resulted in the following correlation:

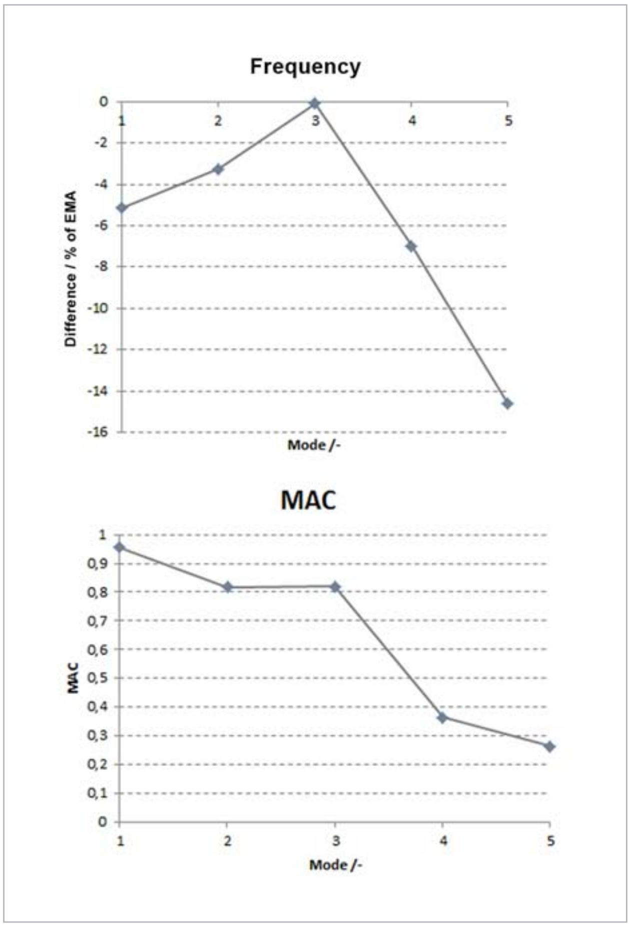

Fig. 4: Comparison of the Experimental Modal Analysis (EMA) with the simulation of the bar

Differences between the initial simulation and measurement can especially be observed in the higher modes. The frequency difference could particularly be improved by optimizing the material parameters of the microstructure.

Sensitivity analysis and optimization

First, the influence of various parameters on the natural frequencies and mode shapes is studied using a sensitivity analysis. The parameters for copper such as Young's modulus, Poisson's ratio, storage modulus, as well as the Poisson's ratio of the resin or geometry values like the wire diameter, are taken from literature.

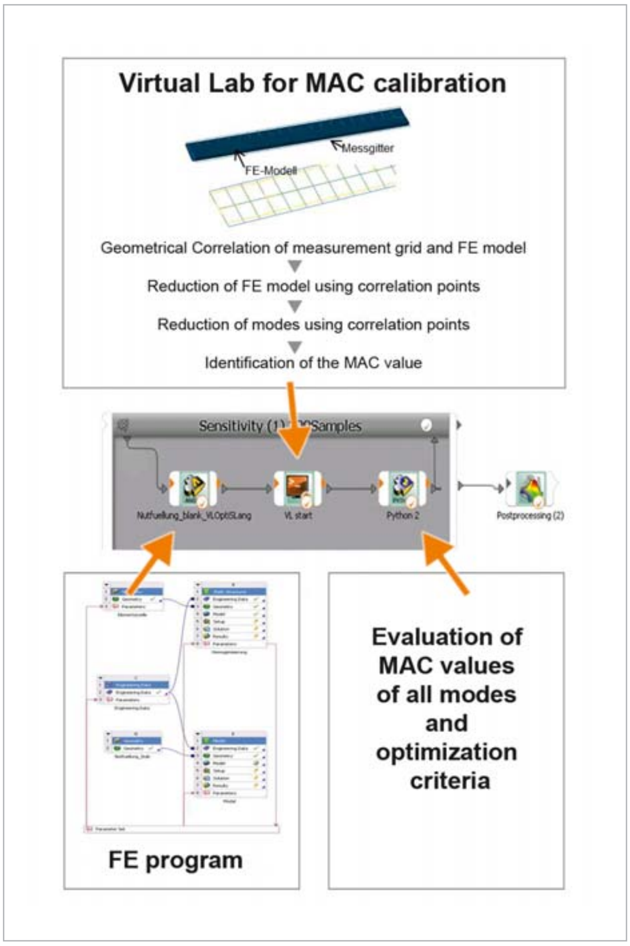

Fig. 5: Workflow overview in optiSLang

For the first five modes, the sensitivity analysis reveals the elastic modulus of resin and copper, as well as the wire diameter to be the main parameters. Here, the elastic modulus of copper and the wire diameters mainly determine the bending modes while the torsional modes are primarily determined by the storage modulus of the resin as well as the wire diameter. Following the sensitivity analysis, an optimization of the main parameters is performed using an Adaptive Response Surface Method (ARSM).

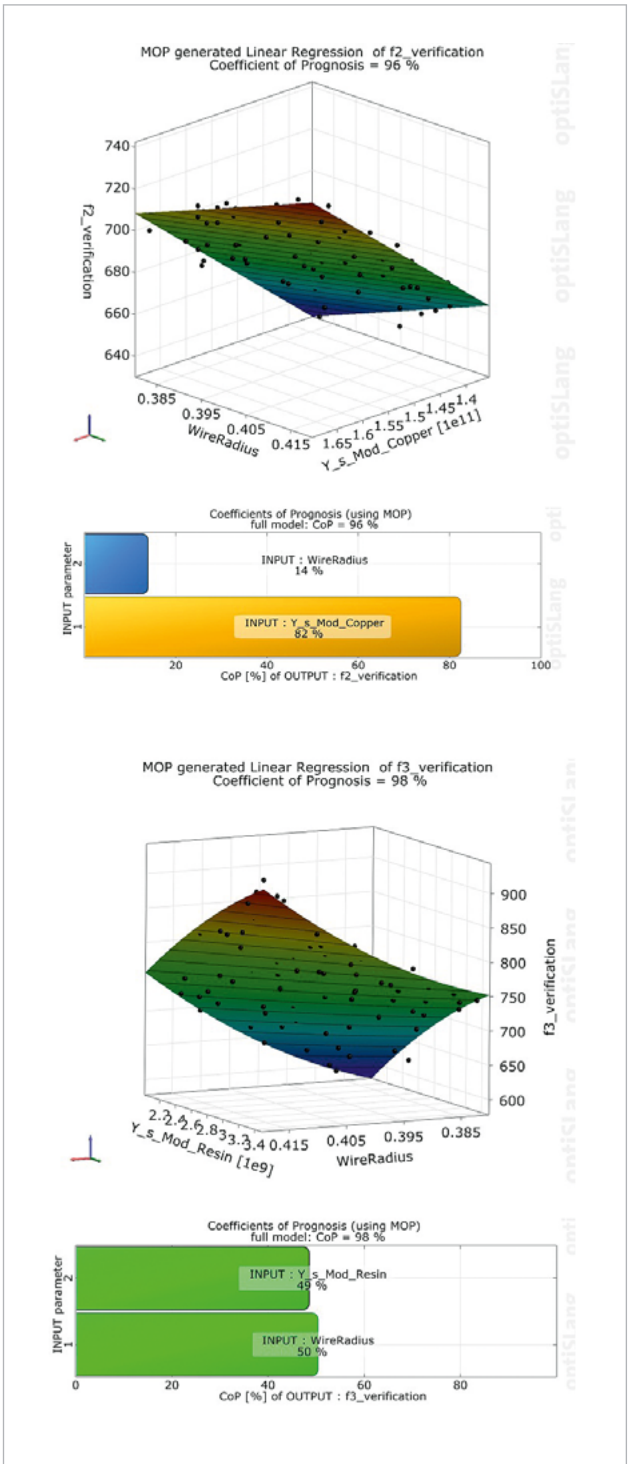

Fig. 6: Metamodel of Optimal Prognosis (MOP) and Coefficient of Prognosis (CoP)

Summary and Results

The results after an optimization of the material parameters show a significant improvement of the frequency and MAC calibration. This method allows an optimal idealization of the windings yielding an improved result quality in the simulation of stator behavior.

Author// Marion Ballweg (Siemens AG | Bad Neustadt)

Contact & Distributors

Worldwide

Dynardo GmbH
Steubenstraße 25
99423 Weimar
Phone: +49 (0)3643 9008-30
Fax.: +49 (0)3643 9008-39
www.dynardo.de
contact@dynardo.de

Dynardo Austria GmbH
Office Vienna
Wagenseilgasse 14
1120 Vienna
www.dynardo.at
contact@dynardo.at

Worldwide distribution of ANSYS optiSLang
ANSYS, Inc.
Canonsburg
www.ansys.com

Worldwide distribution of optiSLang
LightTrans GmbH
Jena
www.lighttrans.de

Germany
CADFEM GmbH
Grafing b. München
www.cadfem.de

Austria
CADFEM (Austria) GmbH
Vienna
www.cadfem.at

Switzerland
CADFEM (Suisse) AG
Aadorf
www.cadfem.ch

Czech Republic, Slovakia, Hungary
SVS FEM s.r.o.
Brno-Židenice
www.svsfem.cz

Sweden, Denmark, Finland, Norway
EDR & Medeso AB
Västerås
www.edrmedeso.com

United Kingdom of Great Britain and Northern Ireland
CADFEM UK CAE Ltd
Croydon, Surrey
www.cadfemukandireland.com

Ireland
CADFEM Ireland Ltd
Dublin
www.cadfemukandireland.com

Turkey
FIGES A.S.
Istanbul
www.figes.com.tr

North Africa
CADFEM Afrique du Nord s.a.r.l.
Sousse
www.cadfem-an.com

Russia
CADFEM CIS
Moscow
www.cadfem-cis.ru

India
CADFEM Engineering Services India
Hyderabad
www.cadfem.in

USA

CADFEM Americas, Inc.
Farmington Hills, MI
www.cadfem-americas.com

Ozen Engineering Inc.
Sunnyvale, CA
www.ozeninc.com

USA/Canada
SimuTech Group Inc.
Rochester, NY
www.simutechgroup.com

Japan
TECOSIM Japan Limited
Saitama
www.tecosim.co.jp

Korea
TaeSung S&E Inc.
Seoul
www.tsne.co.kr

China
PERA-CADFEM Consulting Inc.
Beijing
www.peraglobal.com

Publication details

Publisher
Dynardo GmbH
Steubenstraße 25
99423 Weimar
www.dynardo.de
contact@dynardo.de

Executive Editor & Layout
Henning Schwarz
henning.schwarz@dynardo.de

Registration
Local court Jena: HRB 111784

VAT Registration Number
DE 214626029

Publication
worldwide

© Images
Wikimedia Commons: Eurojet EJ200, cover & p. 2
Fotolia: mihaela19750405, cover & p. 2 | JustContributor, cover & p. 2 | CLIPAREA.com, p. 18 | ArenaCreative, p. 26 | Evgeny Korshenkov, p. 32